

Aus der Klinik für Neurologie  
des Universitätsklinikums Düsseldorf der Heinrich-Heine-Universität  
Direktor: Univ.-Prof. Dr. med. Hans-Peter Hartung

**Future diagnostic and therapeutic perspectives in rare  
neuroinflammatory, neurovascular and neurodegenerative diseases**

Habilitationsschrift  
zur Erlangung der *venia legendi*  
für das Fach Neurologie  
an der Hohen Medizinischen Fakultät  
der Heinrich-Heine-Universität Düsseldorf

Vorgelegt von  
Dr. med. Marius Ringelstein  
Düsseldorf 2016

**Eidesstattliche Erklärung:**

Ich versichere an Eides statt, dass ich die vorliegende Habilitationsschrift ohne unerlaubte Hilfe angefertigt habe, dass ich das benutzte Schrifttum vollständig erwähnt habe und dass die Habilitationsschrift noch von keiner anderen Fakultät abgelehnt worden ist.

Desweiteren versichere ich, dass bei den wissenschaftlichen Untersuchungen, die Gegenstand dieser schriftlichen Habilitationsleistung sind, ethische Grundsätze und die jeweils gültigen Empfehlungen zur Sicherung guter wissenschaftlicher Praxis beachtet wurden.

Dr. med. Marius Ringelstein

Düsseldorf, den 07.01.2016

**This cumulative thesis bases on the following raw data studies:**

1. Oberwahrenbrock T\*, Schippling S\*, **Ringelstein M\***, Kaufhold F, Zimmermann H, Keser N, Young KL, Harmel J, Hartung HP, Martin R, Paul F, Aktas O, Brandt AU. Retinal damage in multiple sclerosis disease subtypes measured by high-resolution optical coherence tomography. *Mult Scler Int* 2012 July;2012:530305.
2. Albrecht P\*, **Ringelstein M\***, Muller AK, Keser N, Dietlein T, Lappas A, Foerster A, Hartung HP, Aktas O\*, Methner A\*. Degeneration of retinal layers in multiple sclerosis subtypes quantified by optical coherence tomography. *Mult Scler* 2012 October;18(10):1422-9.
3. Oberwahrenbrock T\*, **Ringelstein M\***, Jentschke S, Deuschle K, Klumbies K, Bellmann-Strobl J, Harmel J, Ruprecht K, Schippling S, Hartung HP, Aktas O, Brandt AU, Paul F. Retinal ganglion cell and inner plexiform layer thinning in clinically isolated syndrome. *Mult Scler* 2013 December;19(14):1887-95.
4. **Ringelstein M\***, Albrecht P\*, Sudmeyer M, Harmel J, Muller AK, Keser N, Finis D, Ferrea S, Guthoff R, Schnitzler A, Hartung HP, Methner A\*, Aktas O\*. Subtle retinal pathology in amyotrophic lateral sclerosis. *Ann Clin Transl Neurol* 2014 April;1(4):290-7.
5. **Ringelstein M**, Kleiter I, Ayzenberg I, Borisow N, Paul F, Ruprecht K, Kraemer M, Cohn E, Wildemann B, Jarius S, Hartung HP, Aktas O\*, Albrecht P\*. Visual evoked potentials in neuromyelitis optica and its spectrum disorders. *Mult Scler* 2014 April;20(5):617-20.
6. **Ringelstein M**, Metz I, Ruprecht K, Koch A, Rappold J, Ingwersen J, Mathys C, Jarius S, Bruck W, Hartung HP, Paul F, Aktas O. Contribution of spinal cord biopsy to diagnosis of aquaporin-4 antibody positive neuromyelitis optica spectrum disorder. *Mult Scler* 2014 June;20(7):882-88.
7. **Ringelstein M\***, Ayzenberg I\*, Harmel J, Lauenstein AS, Lensch E, Stögbauer F, Hellwig K, Ellrichmann G, Stettner M, Chan A, Hartung HP, Kieseier B, Gold R, Aktas O\*, Kleiter I\*. Long-term Therapy With Interleukin 6 Receptor Blockade in Highly Active Neuromyelitis Optica Spectrum Disorder. *JAMA Neurol* 2015 July;72(7):756-63.
8. **Ringelstein M\***, Albrecht P\*, Kleffner I, Bühn B, Harmel J, Müller AK, Finis D, Guthoff R, Bergholz R, Duning T, Krämer M, Paul F, Brandt A, Oberwahrenbrock T, Mikolajczak J, Wildemann B, Jarius S, Hartung HP, Aktas O\*, Dörr J\*. Retinal pathology in Susac syndrome detected by spectral-domain optical coherence tomography. *Neurology* 2015 August;85(7):610-8.

\*equally contributing first and senior authors

## List of contents

1. Introduction.....	3
2. Optical coherence tomography.....	5
3. Retinal anatomy.....	6
4. Assessment of retinal structures with SD-OCT.....	7
4.1. Retinal nerve fiber layer and total macular volume.....	7
4.2. Deeper retinal layers.....	8
5. Clinical application of OCT.....	9
6. Multiple Sclerosis.....	9
6.1. OCT in Multiple Sclerosis.....	10
6.2. OCT in subtypes of Multiple Sclerosis.....	10
6.3. OCT of the deeper retinal layers in Multiple Sclerosis patients.....	16
6.4. OCT in clinically isolated syndrome.....	20
7. Amyotrophic lateral sclerosis.....	24
7.1. OCT in Amyotrophic lateral sclerosis.....	25
8. Susac Syndrome.....	28
8.1. OCT in Susac Syndrome.....	29
9. Neuromyelitis optica.....	35
9.1. Contribution of spinal cord biopsies to the diagnosis of NMOSD.....	37
9.2. Visual evoked potentials in NMOSD .....	41
9.3. Current treatment options in NMOSD.....	47
9.4. Tocilizumab treatment in NMOSD.....	47
10. Summary, conclusion and outlook.....	52
11. German Summary (Zusammenfassung).....	54
12. Acknowledgement.....	59
13. Reference list.....	60

## 1. Introduction

Most diseases of the central nervous system (CNS) including neuroinflammatory, neurovascular and primarily neurodegenerative disorders are characterized by stage-dependent axonal and/or neuronal cell loss, that is usually not reversible, but possibly preventable. The detection of the magnitude of neuro-axonal degeneration is essential to evaluate both the disease progress, associated with functional loss, as well as the efficacy of therapeutic interventions, rendering reliable biomarkers and diagnostic tools essential for clinical practice.

Possible molecular biomarkers in neurodegenerative diseases such as the neurofilament heavy-chain NfH<sup>SM135</sup> in amyotrophic lateral sclerosis (ALS) [Brettschneider et al. 2006], phosphorylated tau epitopes in Alzheimer's disease [Hempel et al. 2003], as well as protein deglycase DJ-1 and/or  $\alpha$ -synuclein in Parkinson's Disease [Hong et al. 2010] were detected in the cerebrospinal fluid (CSF), but are not yet routinely used as diagnostic or prognostic markers due to insufficient reproducibility, or low sensitivity and specificity. Neuroimaging techniques such as magnetic resonance imaging (MRI) with voxel-based morphometry, spectroscopy or diffusion tensor imaging (DTI), or positron emission tomography (PET) and single photon emission computed tomography (SPECT) are in general use in order to visualize and quantify neurodegenerative processes of the brain in relation to functional aspects [Price et al. 2004; McEvoy et al. 2009; Ramli et al. 2015; Habeck et al. 2008; Parisi et al. 2014]. They are, however, often not routinely available, time-consuming and expensive. Hence, their systematic use is mostly restricted to trials or other selected research issues.

Similarly, in the light of economic aspects, the general interest in so-called "rare diseases" (in the European Union defined as diseases with a prevalence of < 5/10.000 inhabitants) is rather low, rendering the search for diagnostic tools or biomarkers and novel therapeutic options exceedingly difficult. Thus, easy to apply, non-invasive and worthwhile diagnostics as well as seminal efficient and safe treatments are highly appreciated, particularly in "orphan diseases".

The main part of this work (i.e. the above publications Nos. 1-4 and 8) considers the detection and quantification of neuro-axonal loss in each one of the following disorders, primary neuroinflammatory (Multiple Sclerosis (MS)), neurodegenerative (ALS) and neurovascular (Susac Syndrome (SuS)) diseases by means of optical coherence

tomography (OCT) of the retina, which is a protruded part of the brain. Spectral-domain OCT (SD-OCT) is an easily applicable approach to investigate all types of primary or secondary neuro-retinal disorders with absolute noninvasiveness and histology-like anatomical detail. As functional and structural measures like low contrast visual acuity, visual evoked potentials (VEP) and OCT parameters correlate with e.g. brain atrophy on MRI, quality of life and the degree of disability i.a. in MS patients [Balcer et al. 2015], the visual pathway is an ideal and easy investigatable anatomical structure to detect neurodegeneration of the brain.

The above publications (Nos. 5-7) not only focus on diagnostic aspects (spinal cord biopsy and VEP), but also consider the effects of a promising new therapeutic compound (Tocilizumab) in patients with neuromyelitis optica spectrum disorders (NMOSD). Notably, in contrast to MS [Compston and Coles 2008], ALS [Kiernan et al. 2011], SuS [Dörr et al. 2013a] and NMOSD [Wingerchuk and Weinshenker 2014] are classified as „rare diseases“ with prevalences below 1 per 10.000 inhabitants.

With the research studies presented in detail below we aimed to answer the following three questions regarding innovative diagnostic work-up approaches and a promising therapeutic option in different, mostly “orphan” neuroinflammatory, neurodegenerative and neurovascular diseases:

1. Can SD-OCT reliably detect neuro-axonal loss in primary neuroinflammatory (MS), neurodegenerative (ALS) and neurovascular (SuS) disorders and can SD-OCT help to differentiate these diseases, e.g. SuS from MS?
2. What is the (differential-) diagnostic contribution of spinal cord biopsy and VEP in NMOSD patients?
3. Is the long-term Interleukin-6 receptor blockade with Tocilizumab an effective and safe treatment alternative for highly disease-active NMOSD patients?

To answer these questions we investigated the so far largest cohorts of patients with different MS subtypes, definite ALS and SuS by means of SD-OCT and compared the patient groups with healthy controls or with each other. Furthermore, for the first time, we retrospectively evaluated the impact of diagnostic spinal cord biopsy and VEP in primarily Caucasian NMOSD patients. Finally, we analyzed the efficacy and safety of Tocilizumab over the longest observation time in the largest cohort of exclusively Caucasian NMOSD patients hitherto published in the literature.

## 2. Optical coherence tomography

Optical coherence tomography (OCT), first described by Huang and colleagues in 1991 [Huang et al. 1991], is a non-invasive technique using low-coherence interferometry to obtain cross-sectional or three-dimensional images of the retina as remote part of the brain. OCT can be considered an optical analogue of the B-mode ultrasonography and allows a precise morphological examination of the retinal layered microarchitecture [Drexler et al. 2001]. Low coherence infrared light (800-1400 nm) is emitted from a superluminescence diode and is split into 2 compounds by a fiberoptic splitter: one part is reflected by a reference mirror, the other part enters the eye and is reflected from the retinal structures (Figure 1). The magnitude and the echo time delay of both back-scattered compounds are detected by a photodetector in the interferometer, then processed and finally visualized. Because the path length of the reference mirror is known, it is possible to calculate the depth of the reflecting tissue from this time delay. Thus, the amplitude of the reflection can be expressed on a decibel scale as a function of the depth of the reflecting tissue, to produce an axial scan (A-scan) of the retina. Multiple adjacent A-scans can be combined to produce cross-sectional (B-scan) as well as three-dimensional images.

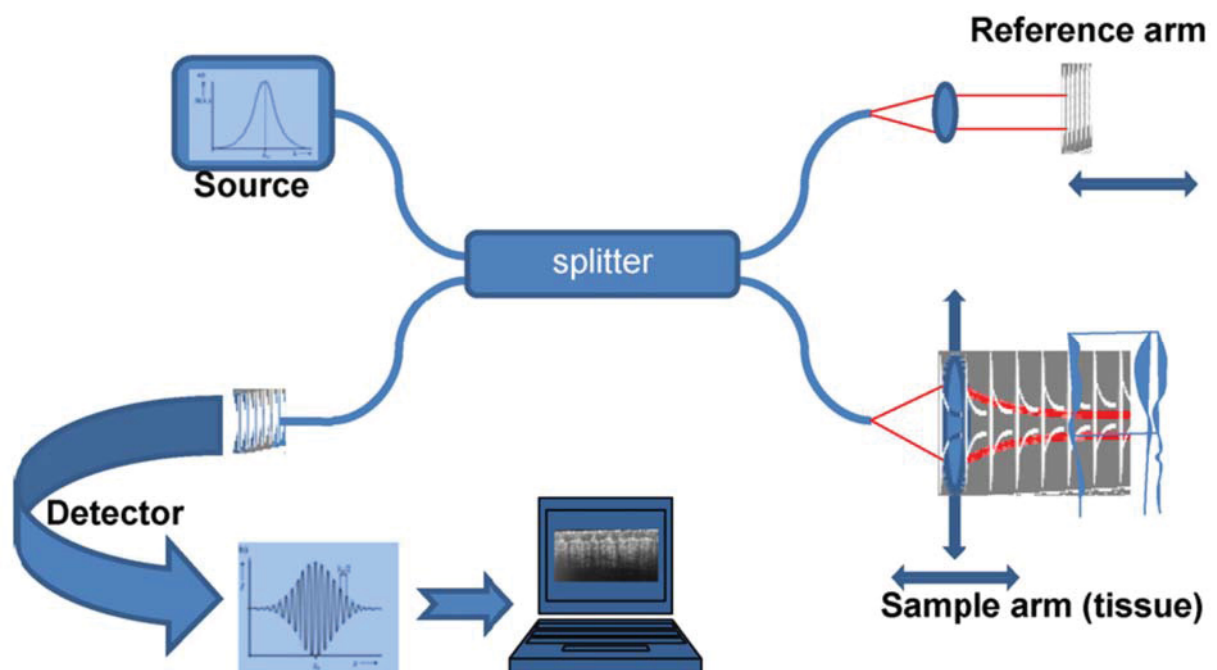


**Figure 1:** *Technical principle of optical coherence tomography* (from [Cauberg et al. 2009]). Low coherence infrared light is emitted from a superluminescence diode ("source") and is split into 2 compounds by a fiberoptic "splitter": one part is reflected by a reference mirror, the other

part by the sample tissue. The magnitude and the echo time delay of both back-scattered compounds are detected by a photodetector and then further processed.

Two types of OCT technology are currently available, both based on the interferometer principle, but differing in the way in which the reflected lights are processed. 1. The time domain-OCT (TD-OCT) is based on the *time difference* between the reflections in the two arms, 2. The spectral domain-OCT (SD-OCT) is based on the interference patterns in a *spectrum of mixed reflected* light, which are analyzed by a spectrophotometer. Thus, SD-OCT allows for a higher data acquisition speed (29.000 vs. 400 A-scans/s) and a higher axial resolution of approximately 2  $\mu\text{m}$  with SD-OCT vs. 10  $\mu\text{m}$  with TD-OCT and is suitable for three-dimensional scans and video imaging.

### **3. Retinal Anatomy**

From an evolutionary point of view, the retina is a very peripherally situated part of the brain. Below the inner limiting membrane, the retinal nerve fiber layer (RNFL) contains the axons of the ganglion cells, which then continue to form the optic nerves, the chiasm, and optic tracts. Since retinal axons are non-myelinated until they penetrate the lamina cribrosa, the RNFL is an ideal structure to visualize processes of axonal neurodegeneration, both in their natural setting but also as a consequence and marker of neuroprotective interventions. The cell bodies of the RNFL are located in the ganglion cell layer (GCL), which is synaptically connected by the inner plexiform layer (IPL) to the inner nuclear layer (INL), which contains specialized interneurons, so called horizontal, bipolar, and amacrine cells. The outer plexiform layer (OPL) connects the INL with the outer nuclear layer (ONL) in which the nuclei and cell bodies of the light-sensitive photoreceptor cells (rods and cones) are located (Figure 2).

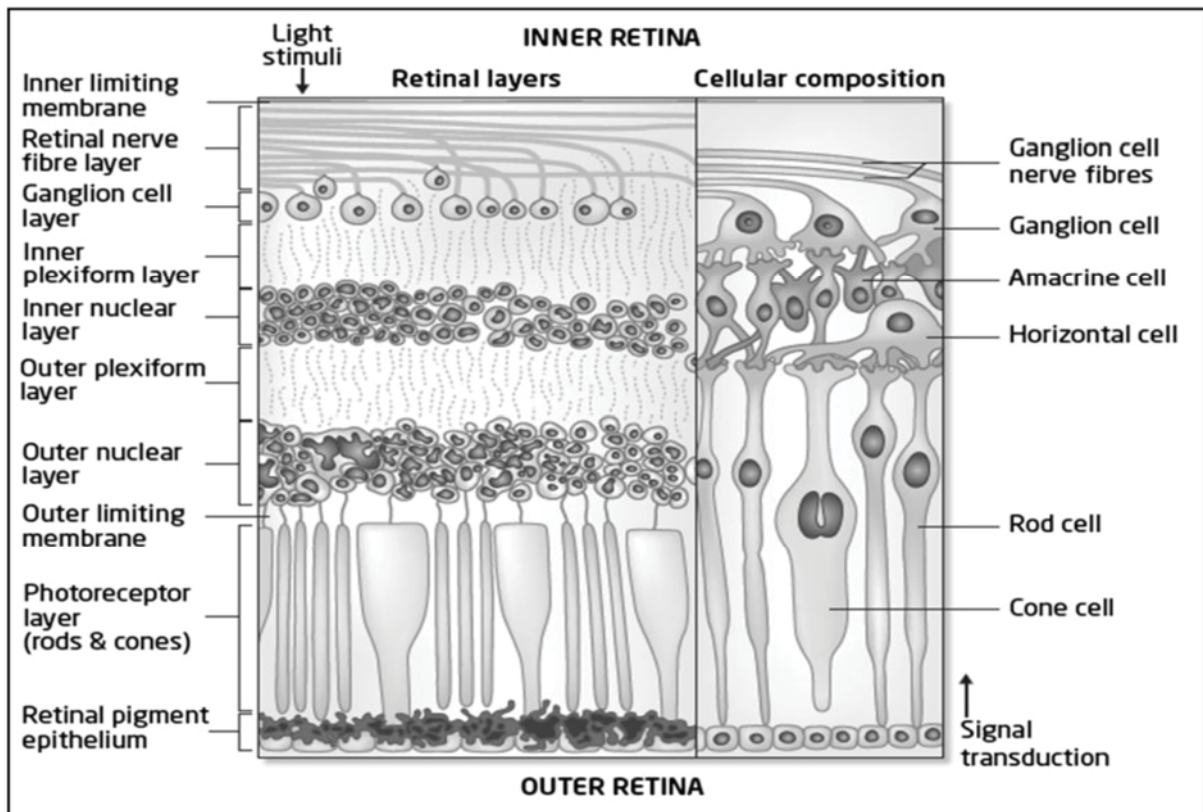


**Figure 2:** Schematic cross-sectional illustration of the retinal anatomy (from [Saidha et al. 2011]). Below the inner limiting membrane, unmyelinated axons in the retinal nerve fiber layer originating from the ganglion cells (in the ganglion cell layer) are synaptically connected by the inner plexiform layer to the inner nuclear layer, that contains the cell bodies and nuclei of the horizontal, bipolar, and amacrine cells. These are synaptically connected by means of the outer plexiform layer to the light sensitive photoreceptor cells (rods and cones) with their nuclei and cell bodies located in the outer nuclear layer.

#### 4. Assessment of retinal structures with SD-OCT

##### 4.1. Retinal nerve fiber layer and total macular volume

Using the latest generation Spectralis SD-OCT device with image alignment eye tracking-software (TruTrack, Heidelberg Engineering, Heidelberg, Germany), the peripapillary RNFL (pRNFL) was measured in our studies by a 12° circular scan with a diameter of approximately 3.4 mm (composed of 1024 A-scans), centered on the optic nerve head (Figure 3A). To obtain the total macular volume (TMV), perifoveal volumetric retinal scans using a common 1, 3, and 6 mm Early Treatment Diabetic Retinopathy Study (ETDRS) grid, consisting of 25-61 vertical B-scans (scanning angles = 15° × 15° up to 30° × 25°), and focusing the fovea centralis were performed

(Figure 3B). The mean pRNFL and the TMV were automatically evaluated by the Heidelberg Eye Explorer software.

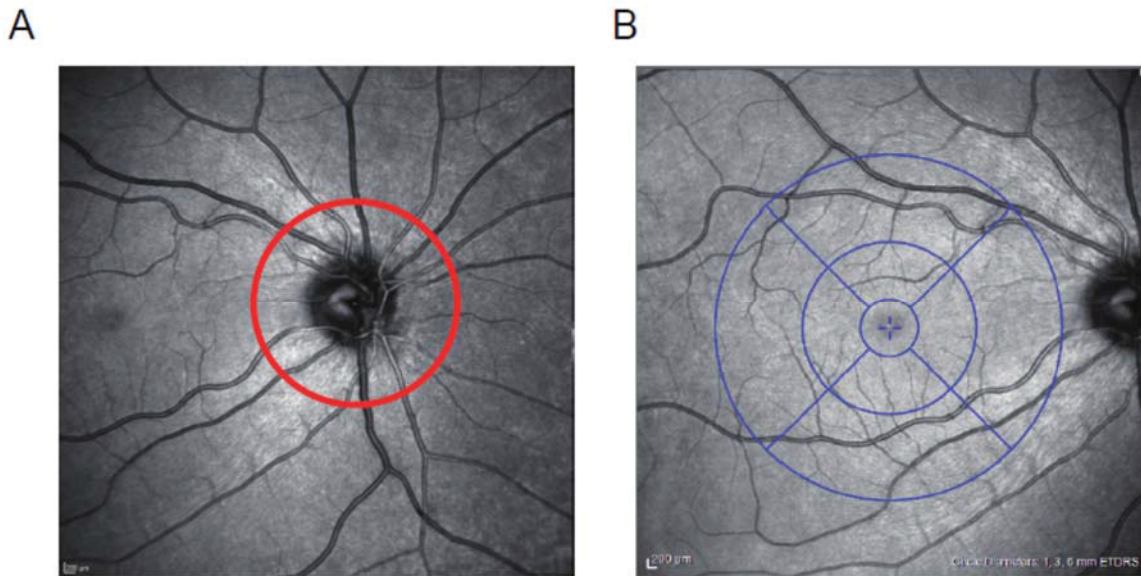


**Figure 3:** Assessment of the peripapillary retinal nerve fiber layer and the total macular volume with SD-OCT. The mean peripapillary retinal nerve fiber layer (RNFL) was measured in a circular 12° scan centered on the optic nerve head (A). The total macular volume (TMV) was evaluated by a volumetric retinal scan using the 1, 3, and 6 mm ETDRS grid (blue circles; B) (from [Ringelstein *et al.* 2015a]; see above publication No. 8).

#### 4.2. Deeper retinal layers

To measure the thickness of the macular RNFL (mRNFL) and the deeper retinal layers single high resolution cross-sectional B-scans, averaged from 100 images, were *manually* or *automatically* (Heidelberg Engineering software, Version 1.7.1.0) segmented by positioning lines on the borders of the different layers (Figure 4).

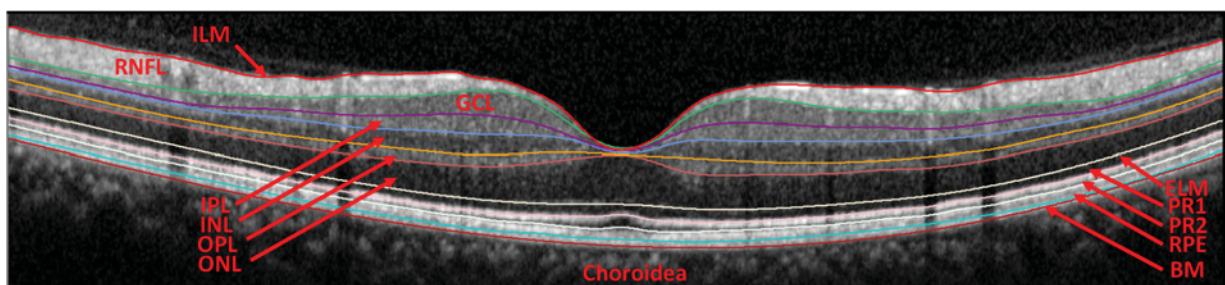


**Figure 4:** Assessment of the parafoveal inner retinal layers within a high-resolution cross-sectional SD-OCT scan. Colored lines were manually or semi-automatically positioned on the borders of the different layers to precisely divide them from each other. ILM = inner limiting

membrane, RNFL = retinal nerve fiber layer, GCL = ganglion cell layer, IPL = inner plexiform layer, INL = inner nuclear layer, OPL = outer plexiform layer, ONL = outer nuclear layer, ELM = External limiting membrane, PR1/2 = inner/outer photoreceptors, RPE = retinal pigment epithelium, BM = Bruch's membrane (from [Ringelstein et al. 2015a]; see above publication No. 8).

## **5. Clinical application of OCT**

First methodologically described by Huang and colleagues in 1991 [Huang et al. 1991], OCT was initially used in vivo in 1993 to investigate the retina [Swanson et al. 1993] and the anterior segment of the human eye [Izatt et al. 1994]. In the mid-nineties first clinical OCT studies were conducted by ophthalmologists, where OCT turned out to be a powerful tool for detecting and monitoring a variety of macular disorders [Puliafito et al. 1995] and to quantitatively assess the thickness of the RNFL [Schuman et al. 1995]. First clinical applications of OCT in neurological diseases date back to 1999 and 2001 by Parisi and colleagues who provided evidence of a significant RNFL thickness reduction in eyes of Multiple Sclerosis (MS) patients with a previous history of optic neuritis (ON) [Parisi et al. 1999], but also in patients with Alzheimer's disease, when compared to healthy controls [Parisi et al. 2001].

We and other groups were able to characterize distinct retinal alterations in various neurological diseases of vascular origin e.g. in cerebral autosomal dominant arteriopathy with subcortical infarcts and leucoencephalopathy (CADASIL) [Rufa et al. 2011], after posterior cerebral artery infarctions [Yamashita et al. 2012], or in Moya Moya disease [Albrecht et al. 2015], but also in patients with classical neurodegenerative diseases such as spinocerebellar ataxia type I [Stricker et al. 2011], multiple system atrophy [Fischer et al. 2011] and Parkinson syndromes [Albrecht et al. 2012b], as well as in metabolic disorders like vitamin B12 deficiency [Turkyilmaz et al. 2013] and Wilson's disease [Albrecht et al. 2012a].

## **6. Multiple Sclerosis**

Multiple sclerosis is a chronic inflammatory disease of the CNS based on autoimmune mechanisms targeting both white and gray matter. Its prevalence in Germany is estimated to be approximately 15/10.000 [Hein and Hopfenmuller 2000]. Primary

demyelinating processes with secondary reduction in axonal transmission lead to concomitant axonal and neuronal degeneration that is responsible for chronic progression of and permanent disability from the disease [Hauser et al. 2013; Trapp and Nave 2008; Lucchinetti et al. 2011]. Whereas a vast majority of MS patients presents with a relapsing-remitting disease course (RRMS), subsequently transforming into secondary progressive MS (SPMS), a smaller portion of patients shows a primary progressive disease course (PPMS) from the very beginning [Compston and Coles 2008]. In 50 % of MS patients visual dysfunction is the presenting symptom and optic neuritis in particular is the heralding event in up to 38 % of patients [Arnold 2005; Keltner et al. 2010]. Affection of the visual function occurs in up to 80 % of the patients with longstanding MS, and loss of vision is the second most important deficit causing reduced quality of life [Compston and Coles 2008; Graves and Balcer 2010].

### **6.1. OCT in Multiple Sclerosis**

Several studies had already demonstrated a thinning of the RNFL and a reduction of the TMV in MS patients with and without ON [Burkholder et al. 2009; Brandt et al. 2011; Saidha et al. 2011]. In a meta-analysis of MS studies using TD-OCT, a RNFL thinning in the size of 20.38  $\mu\text{m}$  ( $n=2063$ ,  $p<0.0001$ ) in eyes with previous ON, compared to 7.08  $\mu\text{m}$  ( $n=3154$ ,  $p<0.0001$ ) in eyes without ON was confirmed [Petzold et al. 2010]. RNFL thinning is clinically associated with significant visual loss [Talman et al. 2010] and also correlates with clinical impairment, as well as with paraclinical abnormalities e.g. white matter changes of the brain on MRI [Young et al. 2013]. However, more specific OCT data on distinct MS subtypes (i.e. RRMS vs. SPMS vs. PPMS) using SD-OCT were scarce at that time, and the results were at least in part conflicting.

### **6.2. OCT in subtypes of Multiple Sclerosis**

In this multicenter SD-OCT study performed in Berlin, Düsseldorf and Hamburg, we recruited 414 MS patients, stratified for the different disease subtypes (RRMS:  $n=308$ , SPMS:  $n=65$ , PPMS:  $n=41$ ) as well as 94 healthy controls (HC) for comparison (Table 1) ([Oberwahrenbrock et al. 2012]; see above publication No. 1). For the MS patients, a previous ON had to be verified either by medical records, abnormal VEP or by characteristic patient's self-report. The expanded disability status scale (EDSS) [Kurtzke 1983] was assessed to evaluate the degree of clinical disability.

**Table 1: Demographic and clinical data of MS patients and healthy controls.**

		HC		MS		
			RRMS	SPMS	PPMS	All MS
No. of Subjects	Total	94	308	65	41	414
	Berlin	63	95	22	8	125
	Hamburg	0	158	23	22	203
	Düsseldorf	31	55	20	11	86
No. of Eyes (eyes with ON)	Total	183	561 (156)	116 (27)	77 (0)	754 (183)
	Berlin	122	187 (77)	44 (15)	16 (0)	247 (92)
	Hamburg	0	270 (54)	35 (2)	41 (0)	346 (56)
	Düsseldorf	61	104 (25)	37 (10)	20 (0)	161 (35)
Gender	Male (%)	31 (33)	87 (28)	29 (45)	24 (59)	140 (34)
	Female (%)	63 (67)	221 (72)	36 (55)	24 (41)	274 (66)
Age (in years)	Mean (SD)	34.47 (10.25)	39.10 (9.50)	48.23 (6.11)	46.90 (7.10)	41.31 (9.59)
	Range	19–56	19–58	33–59	32–59	19–59
Disease duration (in months)	Mean (SD)	NA	91.05 (80.26)	186.15 (87.94)	100.02 (93.33)	106.87 (89.51)
	Range	NA	0–384	39–403	4–426	0–426
EDSS	Median	NA	2.0	5.5	4.0	2.5
	Range	NA	0-7	3-8	2-8	0-8

MS patients were subdivided into the subtypes relapsing-remitting MS (RRMS), secondary-progressive MS (SPMS), and primary-progressive MS (PPMS). ON = optic neuritis, NA = not applicable, EDSS = expanded disability status scale (from [Oberwahrenbrock et al. 2012]; see above publication No. 1).

#### *Mean RNFL thickness and TMV in MS patients without previous optic neuritis*

Eyes of MS patients without a previous ON (no ON = NON) showed a significant reduction of both RNFL thickness and TMV compared to HC, independent of the MS subtype ( $P < 0.001$  for all subtypes). When adjusting for age, gender, and disease duration, with Generalized estimating equation (GEE) models, the mean RNFL was significantly thinner in SPMS compared to RRMS eyes ( $P = 0.007$ ), whereas PPMS eyes did not differ from either RRMS or SPMS eyes. The TMV was significantly reduced in SPMS and PPMS compared to RRMS eyes (SPMS:  $P = 0.039$ , PPMS:  $P = 0.005$ ; Figure 5).

The EDSS was inversely correlated with the RNFL thickness in case of all MS subtypes with NON (RRMS-NON:  $P = 0.007$ ; SPMS-NON:  $P = 0.034$ ; PPMS-NON:  $P = 0.006$ ). In contrast, the TMV was only significantly correlated with the EDSS in RRMS-NON eyes ( $P = 0.003$ ), but not in SPMS-NON ( $P = 0.321$ ) or PPMS-NON ( $P = 0.085$ ) eyes.

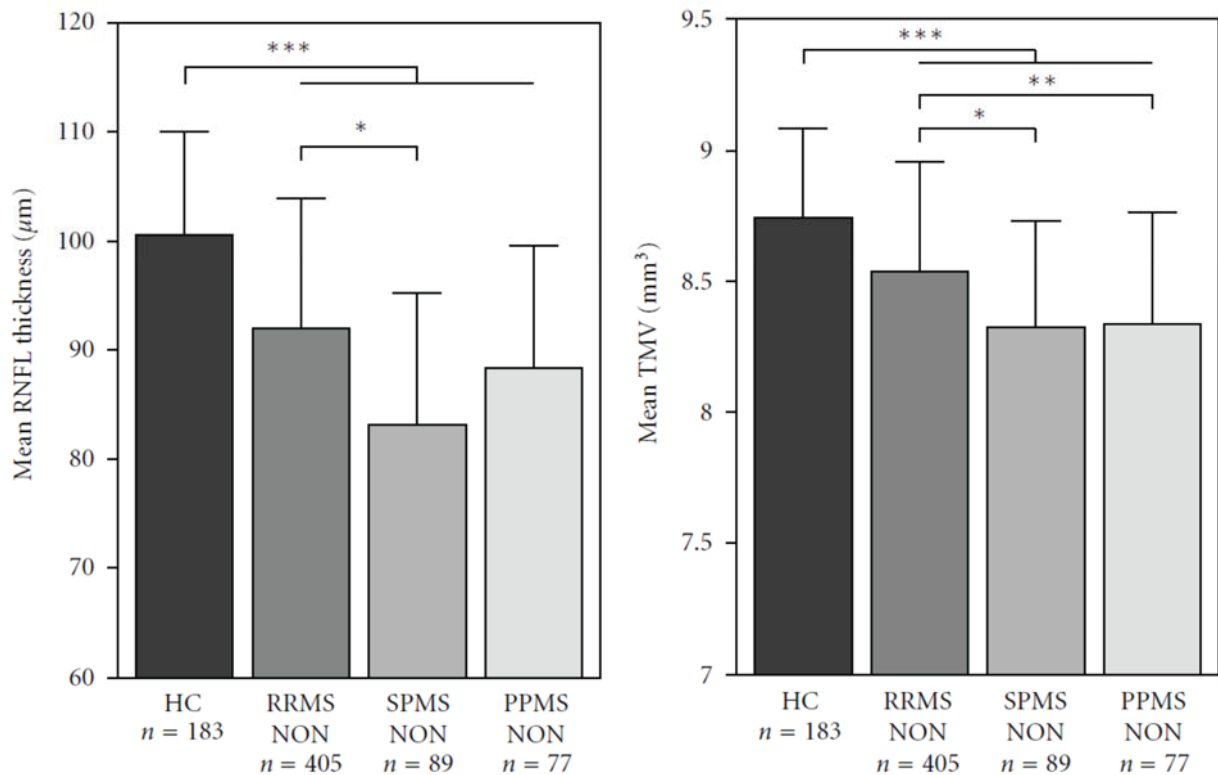


**Figure 5:** *RNFL thickness and TMV in MS patients without previous optic neuritis.* Mean retinal nerve fiber layer (RNFL) thickness and mean total macular volume (TMV) for healthy controls (HC) and MS subtypes (RRMS, SPMS, PPMS) without a history of optic neuritis (NON). Significant differences between the groups are indicated with \* ( $P < 0.05$ ), \*\* ( $P < 0.01$ ) and \*\*\* ( $P < 0.001$ ), respectively (from [Oberwahrenbrock et al. 2012]; see above publication No. 1).

#### *Mean RNFL thickness and TMV in MS patients with previous optic neuritis*

As there were no self-reports or other indications of previous ONs in our PPMS patients, this subgroup was excluded from this analysis. Irrespective of the RRMS/SPMS subtype, MS-ON eyes differed significantly from HC eyes for RNFL thickness and TMV ( $P < 0.001$ , respectively; Figure 6), but no significant differences were detectable between RRMS and SPMS eyes.

RRMS-ON eyes showed a significant inverse correlation between the EDSS and RNFL ( $P = 0.012$ ), while TMV differences did not reach significance ( $P = 0.085$ ). For SPMS-ON eyes no significant correlation of the EDSS with OCT parameters was found (RNFL:  $P = 0.169$ ; TMV:  $P = 0.573$ ).

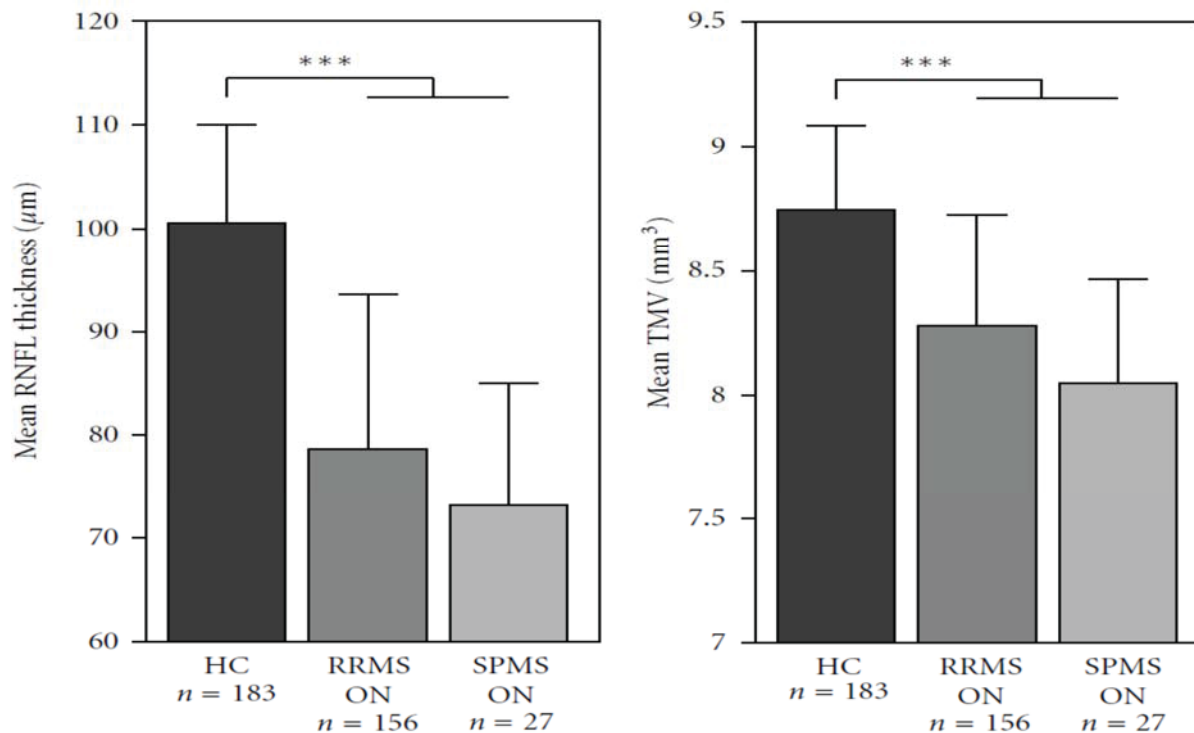


**Figure 6:** RNFL thickness and TMV in MS patients with previous optic neuritis. Mean retinal nerve fiber layer (RNFL) thickness and mean total macular volume (TMV) for healthy controls (HC) and RRMS and SPMS patients with a history of optic neuritis (ON). Significant differences between the groups are indicated with \*\*\* ( $P < 0.001$ ) (from [Oberwahrenbrock et al. 2012]; see above publication No. 1).

#### *Comparison of MS-ON eyes with MS-NON eyes and HC*

The RNFL thickness of RRMS- and SPMS-ON eyes was significantly thinner compared to the RNFL in RRMS- and SPMS-NON eyes, respectively ( $p \leq 0.001$ ). The same was true for the TMV of ON-affected MS eyes, which was significantly reduced, when compared to HC and to unaffected eyes of the same MS subtype ( $p \leq 0.012$ ).

#### *Association with Disease Duration and Yearly Atrophy Estimate*

Although one would not expect retinal atrophy in MS patients without optic nerve involvement, their eyes showed an association of RNFL thickness and TMV with disease duration in the pooled cohort of all MS subtypes (Figure 7). This association was retained significant in RRMS and SPMS eyes for the RNFL thickness only, and in RRMS eyes exclusively for the TMV. Correlations of RNFL and TMV with disease duration were not significant for PPMS-NON eyes. In all MS subtypes the correlation between RNFL thickness, or TMV, respectively, and disease duration was lost in ON

eyes, indicating that ON causes atrophy by its own overriding the atrophy caused by the cerebral MS lesions.

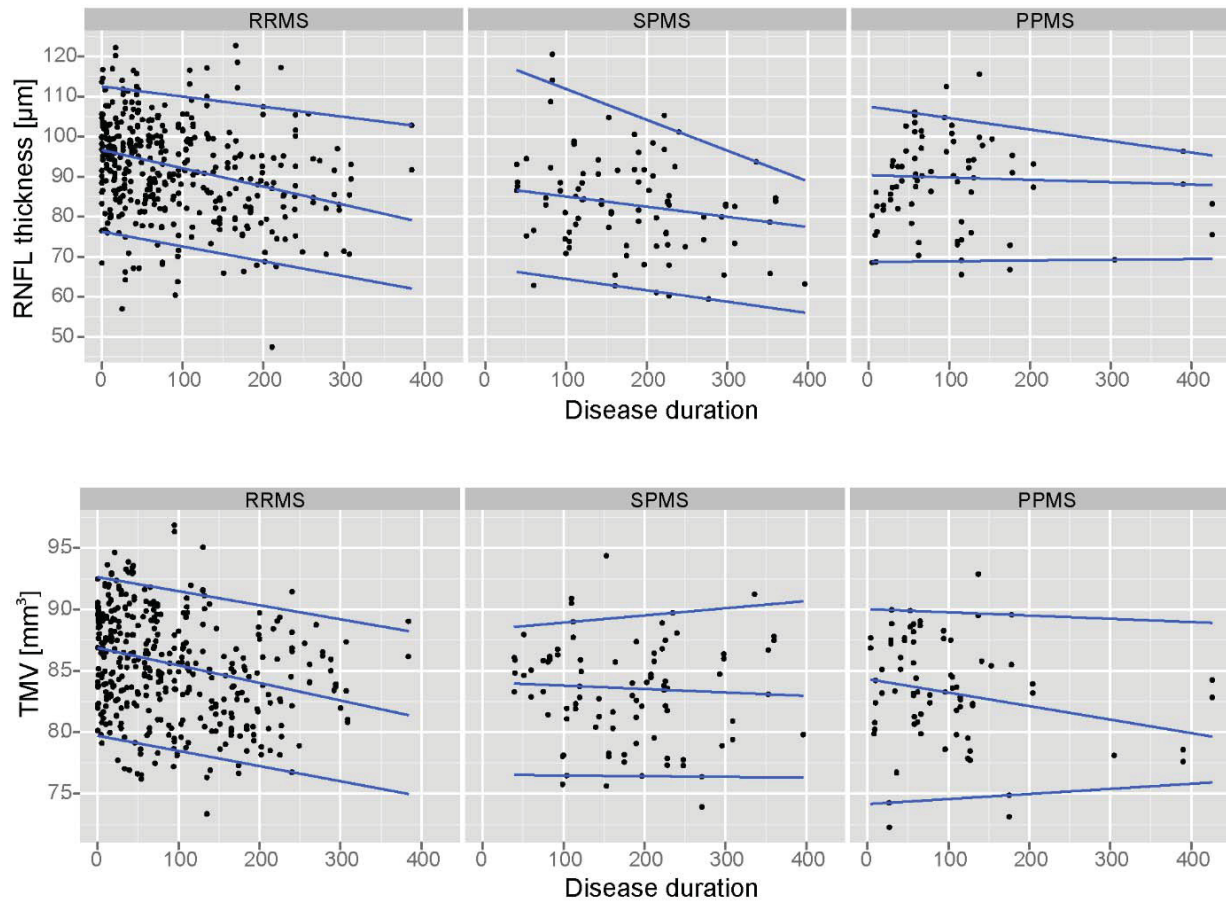


**Figure 7:** Association of the RNFL and TMV with disease duration in MS subtypes. Association of the RNFL thickness and the TMV with disease duration for RRMS, SPMS and PPMS subtypes in eyes without previous optic neuritis. The blue lines indicate the 95%-, 50%- and 5%-quantiles (from [Oberwahrenbrock et al. 2012]; see above publication No. 1).

Based on the effect size of the association of disease duration and RNFL thickness or TMV, we estimated the RNFL thinning and TMV reduction per year of ongoing disease in MS-NON eyes. RRMS-NON eyes showed the strongest and highly significant yearly reduction of RNFL thickness ( $-0.495 \mu\text{m}/\text{year}$ ), and of TMV alike ( $-0.0155 \text{ mm}^3/\text{year}$ ). Interestingly, the significant yearly RNFL thinning in SPMS-NON eyes ( $-0.464 \mu\text{m}/\text{year}$ ) was not concomitantly associated with a significant correlation in TMV change ( $-0.0016 \text{ mm}^3/\text{year}$ ,  $P = 0.838$ ). In contrast, PPMS-NON eyes showed a less pronounced yearly RNFL thinning ( $-0.105 \mu\text{m}/\text{year}$ ), and this occurred in relation to a distinct reduction of TMV ( $-0.0111 \text{ mm}^3/\text{year}$ ).

Hence, in this so far largest ever performed cross-sectional study on retinal atrophy measures in MS subtypes applying latest SD-OCT technology, we showed that both RNFL and TMV are reduced in MS-NON eyes versus HC when pooling all disease subtypes, but also when separately comparing the disease subtypes to HC. Not surprisingly and confirming previous findings, MS-ON eyes exhibited more severe RNFL and TMV damage than MS-NON eyes. The large sample size of our study, however, enabled a statistically robust comparison of various disease subgroups with consideration of confounding factors in the statistical models such as age, disease duration, and gender. The subgroup comparisons revealed a significant reduction of the RNFL thickness in SPMS patients versus RRMS after correction for age, gender, and disease duration and a significant reduction of the TMV in both SPMS and PPMS patients versus RRMS. Of note, like in SPMS, we found a significant reduction of the TMV in NON-eyes of PPMS patients versus RRMS and HC, which may display a generalized neurodegenerative component of PPMS concomitantly reflected through brain atrophy measures [De Stefano et al. 2010].

The time course of RNFL thinning and TMV reduction caused by the atrophy of different retinal layers — be it in the context of ON or independent thereof — is an essential feature of the usefulness of OCT as a biomarker of neuro-axonal loss in longitudinal clinical trials. For MS-ON eyes it had been shown that RNFL thinning occurs within the first 6 months after the ON attack [Trip et al. 2005; Costello et al. 2008], but little was known about temporal dynamics of retinal thinning in MS-NON eyes. Based on published data the yearly retinal atrophy rate in MS is estimated with  $1 \mu\text{m}/\text{year}$ , which is ten times higher, than what can be expected from normal ageing [Petzold et al. 2010]. In PPMS, the MS subtype in which the frequency of ON is lowest, the yearly RNFL thinning was estimated with  $0.12 \mu\text{m}$  (for TMV:  $0.01 \text{ mm}^3$ ) [Henderson et al. 2008], which is in good agreement with our results in PPMS eyes (RNFL thinning  $-0.105 \mu\text{m}/\text{year}$ ; TMV reduction  $-0.011 \text{ mm}^3/\text{year}$ ). In contrast, for RRMS and SPMS patients without ON we estimated higher yearly RNFL changes of nearly  $0.5 \mu\text{m}/\text{year}$ , which is considerably lower than the yearly loss of  $2 \mu\text{m}/\text{year}$  reported in a longitudinal OCT study [Talman et al. 2010], which may be caused i.a. by the different OCT devices applied (TD-OCT in their and SD-OCT in our study).

### **6.3. OCT of the deeper retinal layers in Multiple Sclerosis patients**

Technical advances in the field of SD-OCT with higher resolution imaging subsequently allowed us the in-depth analysis of the deeper retinal layers ([Albrecht et al. 2012c]; see above publication No. 2). As the retinal ganglion cell layer (RGCL) and the IPL were visually still difficult to discriminate at that time, both layers were measured and evaluated together as RGC+IPL complex. We investigated 95 MS patients (RRMS: n=42, SPMS: n=41, PPMS: n=12) with SD-OCT and compared them with 91 age- and sex matched control subjects without ophthalmologic, other inflammatory or degenerative neurological disease.

In addition to the common peripapillary 12° ring scan and the volumetric macular scan to evaluate the pRNFL, and the TMV, respectively, the thickness of the deeper retinal layers was assessed by *manual* segmentation in a single, high resolution cross-sectional scan through the middle of the fovea (averaged from 100 images). The thickness of the different layers was measured at the two thickest points nasally and temporally, except for the ONL, which was measured centrally at its single thickest point. This manual segmentation algorithm was also used in subsequent follow-up studies by our group [Albrecht et al. 2012a; Ringelstein et al. 2014b], and by others as well [Sotirchos et al. 2013].

#### *Mean RNFL thickness and TMV*

As expected, the mean peripapillary RNFL and the mean paramacular thickness in all MS subgroups were thinner, compared to the respective controls. Except for the macular thickness in RRMS patients, these differences were still significant, when only eyes without a history of optic neuritis (HON) were taken into account (Figure 8).

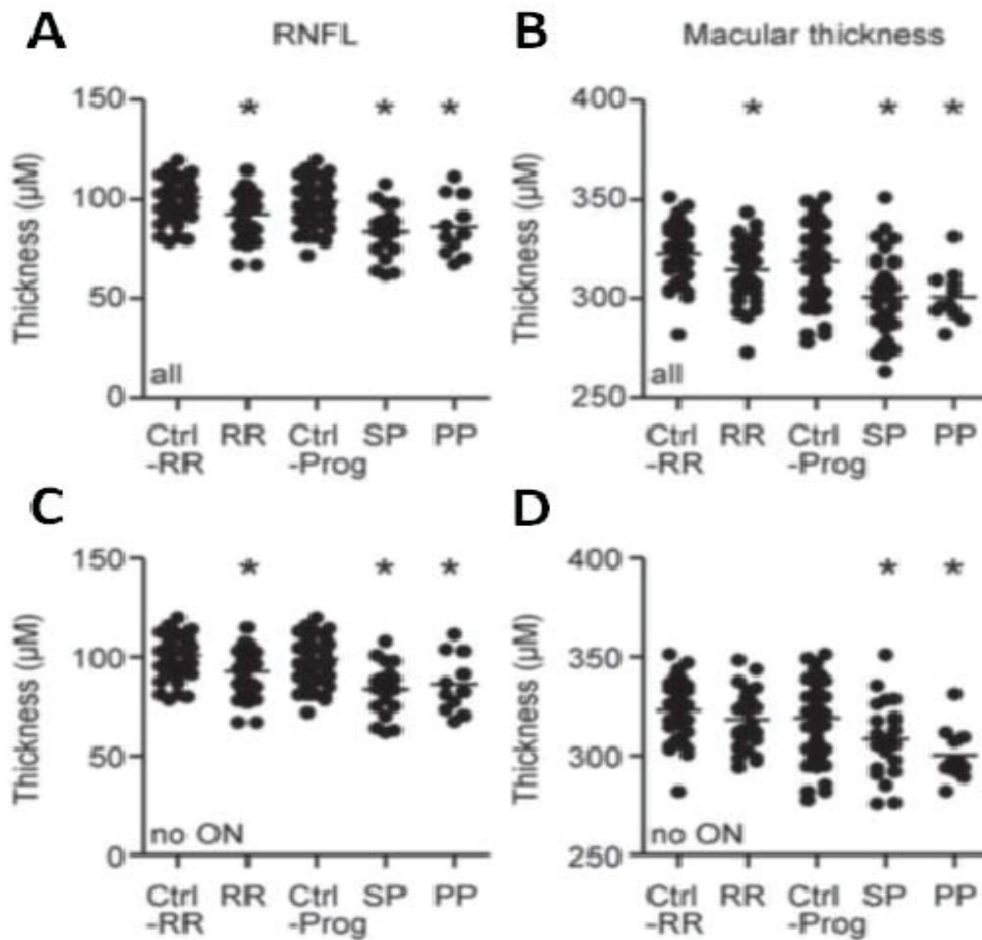


**Figure 8:** Mean RNFL and macular thickness in MS subtypes. Scatter plots display a significant reduction of the peripapillary RNFL (A) and the Macular thickness (B) in all MS patients with and without a history of optic neuritis (HON) compared to controls. Except for the macular thickness in RRMS patients, these significant differences were still evident, when only eyes without HON were taken into account (C+D). Each point represents the mean of the two eyes of one patient. The mean of all patients is indicated by a horizontal bar. Significant differences to the control group are indicated by asterisks ( $p < 0.05$ , ANOVA and Dunnett's post-hoc test) (modified from [Albrecht et al. 2012c]; see above publication No. 2).

#### *Thickness of the different inner retinal layers*

The thickness of the RGC+IPL complex was significantly reduced in the total cohort of all MS subgroups, compared to their respective controls, but more importantly, also in those eyes without previous ON (Figure 9). The thickness of the INL was significantly reduced solely in PPMS eyes, but this reduction was, however, no longer significant when analyzing only eyes without HON. Significant changes of the OPL and the ONL were not observed in any of the MS subgroups.

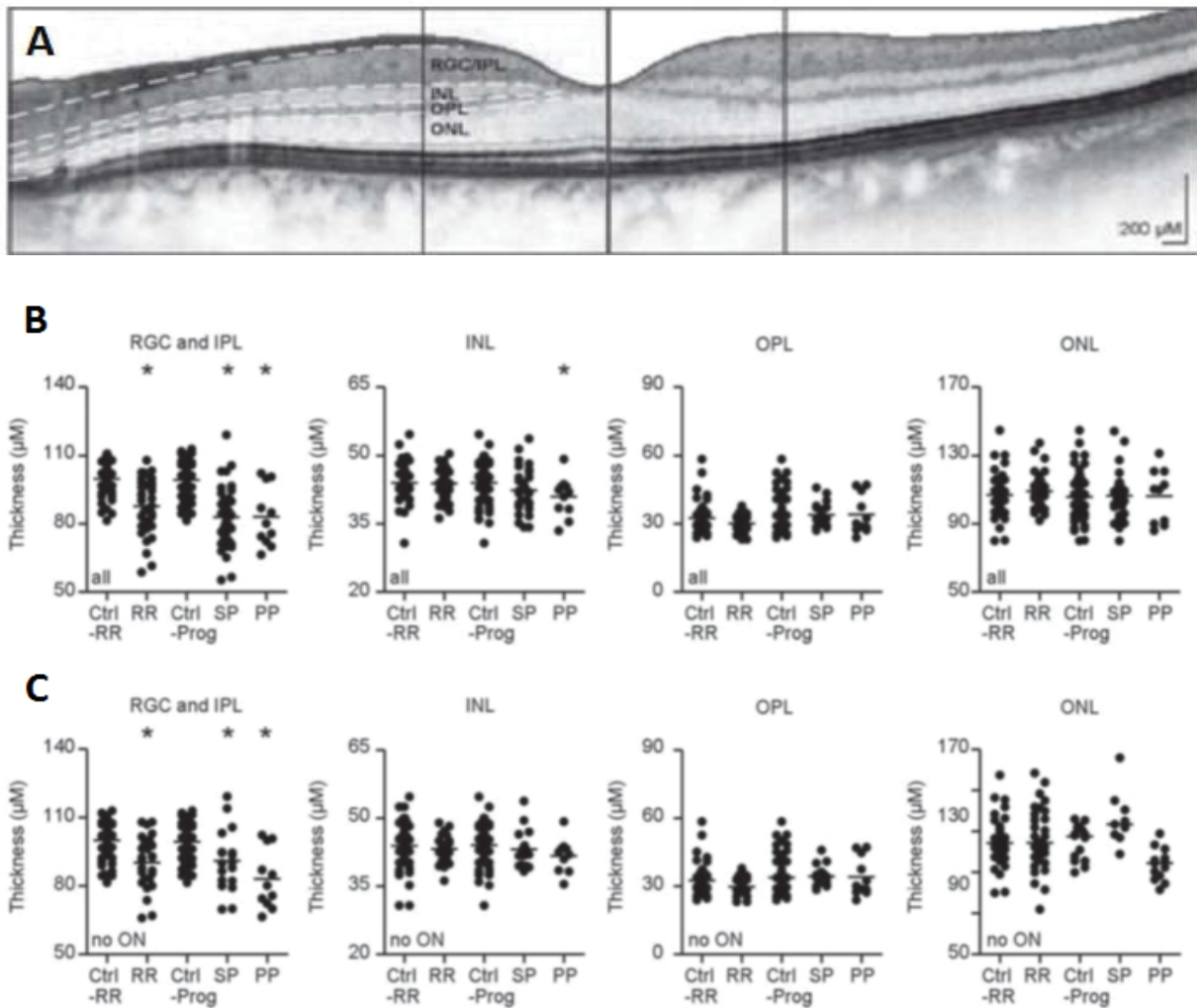


**Figure 9: Manual segmentation of the parafoveal retinal layers.** (A) The segmentation of the different retinal layers was performed manually in single horizontal foveal scans by dividing the retinal layers with white dotted lines. The thickness of all layers was measured at the vertical lines indicating the thickest point nasally and temporally of the fovea, except for the ONL, which was measured centrally along the vertical line. The RGC+IPL complex was significantly reduced in the total (B), as well as in the “no ON” cohort (C) of all MS subgroups, compared to controls, whereas the INL was significantly reduced solely in the entire PPMS eyes. Significant changes of the OPL and ONL were not detectable in any of the MS groups. Each point within the scatter-plots represents the mean of the two eyes of one patient. The mean of all patients is indicated by a horizontal bar. Significant differences to the control group are indicated by asterisks ( $p < 0.05$ , ANOVA and Dunnett’s post-hoc test). RGC+IPL = retinal ganglion cell/ inner plexiform layer complex, INL = inner nuclear layer, OPL = outer plexiform layer, ONL = outer nuclear layer, ON = optic neuritis (modified from [Albrecht et al. 2012c]; see above publication No. 2).

Comparing patient eyes with and without HON revealed a significant reduction of the RNFL, the macular thickness and the RGC+IPL complex in eyes with HON (Figure 10), while no influence of HON was observed in the INL, OPL and ONL. The mean reduction in eyes with HON compared to MS eyes without HON was 7.5  $\mu\text{m}$  for the RNFL, 9  $\mu\text{m}$  for the mean macular thickness, and 7.5  $\mu\text{m}$  for the RGC+IPL.

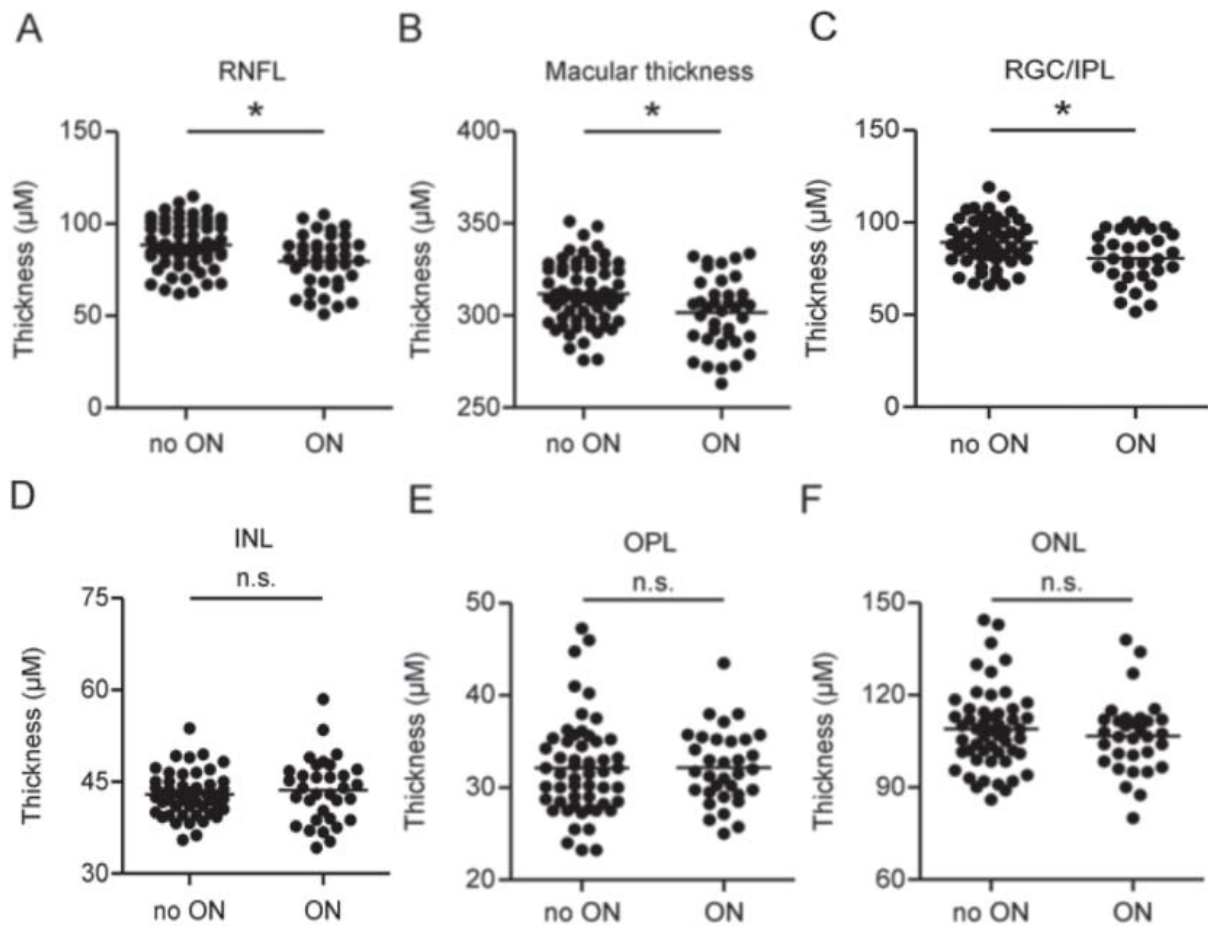


**Figure 10:** Effect of history of optic neuritis on retinal layer thickness. The peripapillary RNFL, the macular thickness and the RGC+IPL complex (A-C), but not the INL, OPL and ONL (D-F) were significantly reduced in eyes with HON compared to those without HON. Each point represents the mean of the two eyes of one patient. The mean of all patients is indicated by a horizontal bar. Significant differences are indicated by asterisks ( $p < 0.05$ , t-test). RNFL = retinal nerve fiber layer, RGC+IPL = retinal ganglion cell/ inner plexiform layer complex, INL = inner nuclear layer, OPL = outer plexiform layer, ONL = outer nuclear layer, ON = optic neuritis, n.s. = not significant (modified from [Albrecht et al. 2012c]; see above publication No. 2).

Taken together, besides the well-known reduction of the RNFL and the macular thickness, this study was one of the first to demonstrate that optic neuritis, and to a

lesser degree, MS without HON, lead to degeneration of the RGC+IPL in all MS subgroups, indicating an axonal (RNFL), but also neuronal (RGC+ILP) cell loss detectable by SD-OCT. The thinning in no-HON eyes can either be attributed to subclinical episodes of ONs not recognized by the patients, or to retrograde trans-synaptic degeneration of the retinal ganglion cells and their axons in the RNFL due to MS lesions of the posterior visual pathways. The additional reduction of the INL thickness, solely in our PPMS patients, is likely to represent a primary retinal pathology, which is independent of inflammatory events of the optic nerve itself. These findings are quite in line with the microscopic study of Green and colleagues who observed atrophy of the INL mainly in eyes of MS patients with progressive multiple sclerosis, while degeneration of the RNFL and the RGC layer was observed in all MS subsets [Green et al. 2010].

#### **6.4. OCT in clinically isolated syndrome**

Because MS usually presents with highest inflammatory activity in the early phase, we investigated patients with clinically isolated syndrome (CIS), the potentially earliest clinical stage, as well as MS patients with less than 2 years since disease onset ([Oberwahrenbrock et al. 2013]; see above publication No. 3). Notably, previous studies applying TD-OCT technology had failed to detect a RNFL or TMV reduction in non-ON eyes of 56 CIS patients compared to HCs [Outteryck et al. 2009], and could not detect retinal damage in fellow eyes of patients with isolated unilateral ON [Kallenbach et al. 2011].

In our study, 45 patients with CIS and 45 age- and sex-matched HCs were prospectively recruited at two university medical centers (Berlin and Düsseldorf). Of these patients, 16 had unilateral ON (six on the right, 10 on the left), 14 presented with spinal cord symptoms, and 6 had experienced relapses suggestive of infratentorial brain lesions. In 7 patients supratentorial signs were found, and one patient exhibited both supratentorial and spinal cord signs. One patient's eye did not pass the quality criteria due to image artefacts. Patients' eyes were stratified into I. eyes with clinical ON (CIS-ON; n = 16), II. eyes with suspected subclinical ON, indicated by VEP latencies of >115ms (CIS-SON; n = 7), and eyes unaffected by ON (CIS-NON; n = 66).

All participants were examined using the peripapillary 12° ring scan to evaluate the pRNFL and a parafoveal macular volume scan comprising 61 vertical B-scans (each with 768 A-Scans, Automatic Real-Time (ART) = 13 frames, scanning angle of 30° ×

25°). Using this data set, the TMV and intra-retinal layer thicknesses were determined within a cylinder of 6 mm in diameter (Figure 11). Of the 61 B-scans, the central B-scan through the fovea and six parallel B-scans each in nasal and temporal direction were automatically segmented and manually corrected in a blinded fashion. For the combined analysis of both eyes, thickness maps of the left eye were mirrored vertically to match the topology of the right eye. The mean thickness maps within each of the study groups were calculated for the macular RNFL (mRNFL), GCL, IPL and INL. The GCL and IPL were again analyzed as single complex (GCIPL).

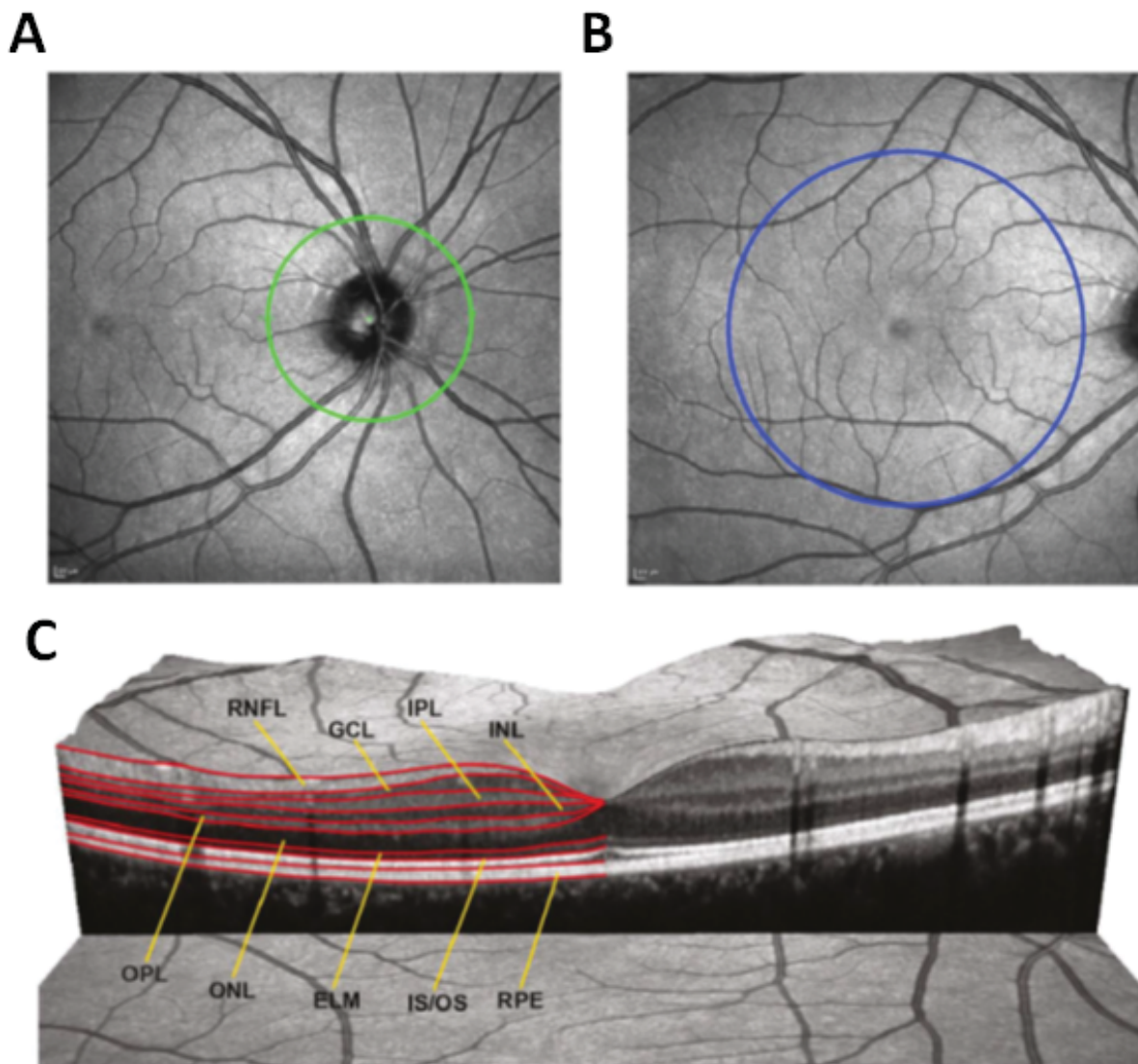


**Figure 11:** *Examples of regions analyzed in OCT.* Scanning laser ophthalmoscopy image showing the peripapillary ring scan to detect the RNFL (green, A), and the blue circle indicating the area for total macular volume and intraretinal layer thickness determination (B). 3D-reconstruction of a macular volume scan, depicting the identified intraretinal layers (C). RNFL = retinal nerve fiber layer; GCL = ganglion cell layer; IPL = inner plexiform layer; INL = inner

nuclear layer; OPL = outer plexiform layer; ONL = outer nuclear layer; ELM = external limiting membrane; IS/OS = inner segments / outer segments; RPE = retinal pigment epithelium (modified from [Oberwahrenbrock et al. 2013]; see above publication No. 3).

### *Peripapillary RNFL and TMV in CIS eyes*

When compared to the corresponding age- and sex-matched controls, the pRNFL thickness was reduced in CIS-ON eyes ( $p < 0.001$ ) and CIS-SON eyes ( $p = 0.014$ ) but not in CIS-NON eyes ( $p = 0.636$ ) (Figure 12). Analysis of macular scans revealed a significant TMV reduction in CIS-ON eyes ( $p < 0.001$ ) and, remarkably, also in CIS-NON eyes ( $p = 0.031$ ) versus controls, but not in the seven CIS-SON eyes.

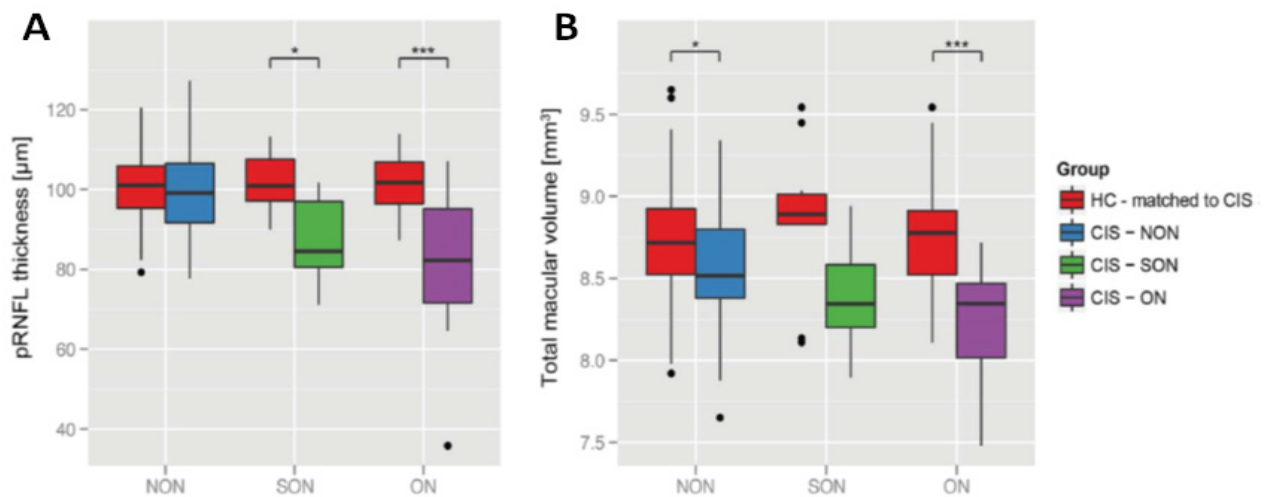


**Figure 12: Peripapillary RNFL and TMV in CIS subgroups.** Significant reduction of the pRNFL thickness in CIS-ON and CIS-SON, but not in CIS-NON eyes (A) and of the TMV in CIS-ON eyes and CIS-NON eyes, but not in CIS-SON eyes compared to HC (B). Significant differences are marked with \* ( $p < 0.05$ ) and \*\*\* ( $p < 0.001$ ). HC = healthy control eyes; CIS-NON = patient eyes without history of ON; CIS-SON = patient eyes without history of ON, but VEP P100 latencies  $> 115$  ms; CIS-ON = patient eyes with clinical ON diagnosis (modified from [Oberwahrenbrock et al. 2013]; see above publication No. 3).

### *Intra-retinal multilayer segmentation*

The analysis of the central macular area showed a significant reduction of the mRNFL thickness in CIS-ON eyes, but not in CIS-SON and CIS-NON eyes in comparison to matched controls. Spatial difference maps showed that the mRNFL thinning was most prominent in close proximity to the optic nerve head, visible but not significant even in CIS-NON eyes (Figure 13). Moreover, all patient groups showed a significantly

reduced GCIPL thickness compared to HCs, particularly in the paramacular region, with the thinning being more pronounced in CIS-ON and CIS-SON eyes than in the CIS-NON group. A supplementary analysis using distinct GCL and IPL thicknesses localized the GCIPL thinning to the GCL in CIS-NON patients. The INL was not significantly altered in all three patient groups compared to HCs.

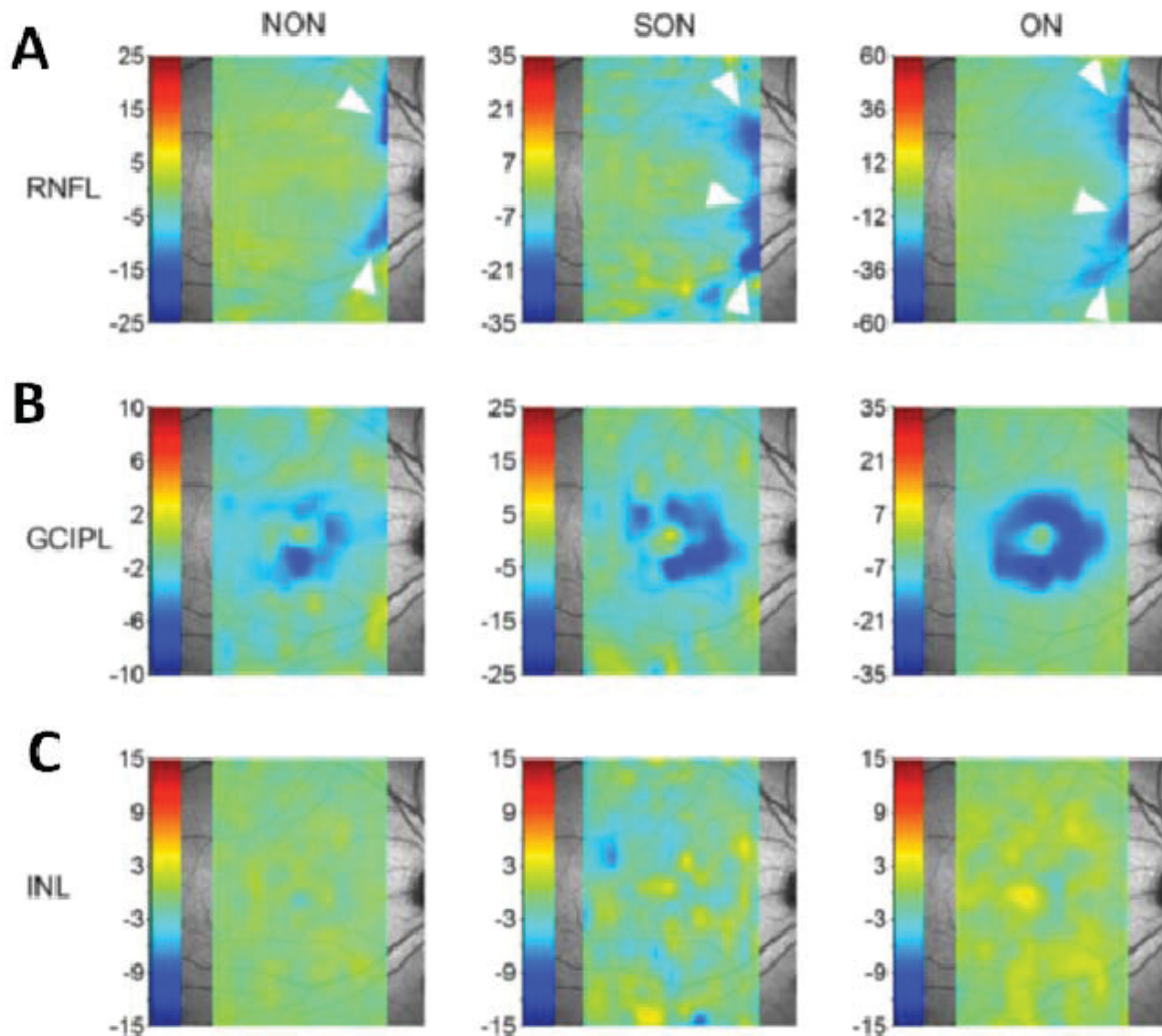


**Figure 13:** *Spatial analysis of changes in CIS eyes versus healthy control eyes.* The mRNFL thickness in CIS-ON eyes, but not in CIS-SON and CIS-NON eyes was significantly reduced in comparison to matched controls with the thinning being most prominent in close proximity to the optic nerve head (A, white arrows). The GCIPL thickness was significantly thinner in the paramacular region in all patient groups compared to HCs, predominantly in CIS-ON and CIS-SON eyes (B). The INL was not significantly altered in all three patient groups compared to HCs (C). RNFL = retinal nerve fiber layer; GCIPL = combined ganglion cell and inner plexiform layer; INL = inner nuclear layer (modified from [Oberwahrenbrock et al. 2013]; see above publication No. 3).

The present study was the first to detect retinal neurodegeneration independent from ON in a large cohort of patients with CIS or early MS by means of SD-OCT. The here detected significant thinning of the GCIPL, mainly due to degeneration of the GCL, in *all* CIS patient groups, as well as the mRNFL reduction exclusively in CIS-ON eyes indicate that retinal *axonal* and *neuronal* damage already occurs in the earliest stages of MS, warranting swift treatment initiation already after the first attack. Our findings corroborate MRI data, that also showed neuro-axonal damage during the very earliest MS stages [Filippi et al. 2003], and corresponding histopathology data from the brain [Lucchinetti et al. 2011] and the eye [Green et al. 2010], as well as findings from experimental autoimmune encephalomyelitis [Fairless et al. 2012]. Furthermore, in line with previous investigations [Syc et al. 2012], our study provides evidence that inflammatory attacks to the optic nerve to the extent of a clinical or subclinical ON may not be a pre-requisite for damage to the retinal GCIPL.

## **7. Amyotrophic lateral sclerosis**

Amyotrophic lateral sclerosis (ALS) is a rare (prevalence < 1/10.000 inhabitants), primarily neurodegenerative disease, characterized by upper and lower motor neuronal loss, resulting in progressive weakness of the limbs as well as the respiratory and bulbar musculature [Kiernan et al. 2011]. Remarkably, autopsy studies such as recent investigations on phosphorylated 43kDa TAR DNA-binding protein (pTDP-43) distribution have shown alterations beyond the pyramidal tract, including the neo- and allocortex, and the basal ganglia [Brettschneider et al. 2013]. In line, extra-motor symptoms occur more frequently in ALS than previously thought and comprise fatigue [Abraham and Drory 2012], pathological laughing and crying [Olney et al. 2011], mild sensory symptoms [Weis et al. 2011] and neuropsychological deficits in the context of overlapping frontotemporal dementia [Byrne et al. 2012]. Moreover, neuro-ophthalmological abnormalities such as nystagmus, defective smooth pursuit or saccadic impairments, as well as decreased high and low contrast visual acuity, were reported [Sharma et al. 2011; Moss et al. 2012]. In this context, studies on VEPs [Munte et al. 1998] and voxel-based MRI volumetry of the occipital cortex revealed functional and structural alterations of the visual system in ALS [Bede et al. 2012].

## 7.1. OCT in Amyotrophic lateral sclerosis

Encouraged by these findings, we used SD-OCT to analyze the possible involvement of the retina in a homogenous monocenter cohort of twenty-four ALS patients. Consecutive patients with “clinically definite” (n=20) or “clinically probable” (n=4) ALS according to the Awaji criteria [Costa et al. 2012] and 24 healthy age- and sex-matched controls were enrolled ([Ringelstein et al. 2014b]; see above publication No. 4). In addition to the common perifoveal volumetric retinal scans to assess the total macular thickness (25 vertical axial scans, scanning area: 6 × 6 mm) and the peripapillary RNFL circular scan, a single high-resolution horizontal scan through the middle of the fovea was manually segmented to measure the deeper retinal layers (Figure 14).

To quantify the segmented layers, two different methods were employed: (1) the mean thickness of the different entire layers was calculated using the Heidelberg Eye Explorer® software, and (2) the thickness of the deeper retinal layers was measured as point estimates (P.E.) at the thickest point nasally and temporally for all layers, except for the ONL, which was measured at the middle of the fovea as previously described above (Figure 14). In so doing, the mean thickness measurement of the complete layers correlated excellently with the P.E. approach for the ganglion cell/inner plexiform layer complex (GCIP; Pearson  $r=0.83$ ,  $p<0.0001$ ), the INL (Pearson  $r=0.87$ ,  $p<0.0001$ ) and the OPL (Pearson  $r=0.89$ ,  $p<0.0001$ ) and acceptably for the ONL (Pearson  $r=0.67$ ,  $p=0.0017$ ).

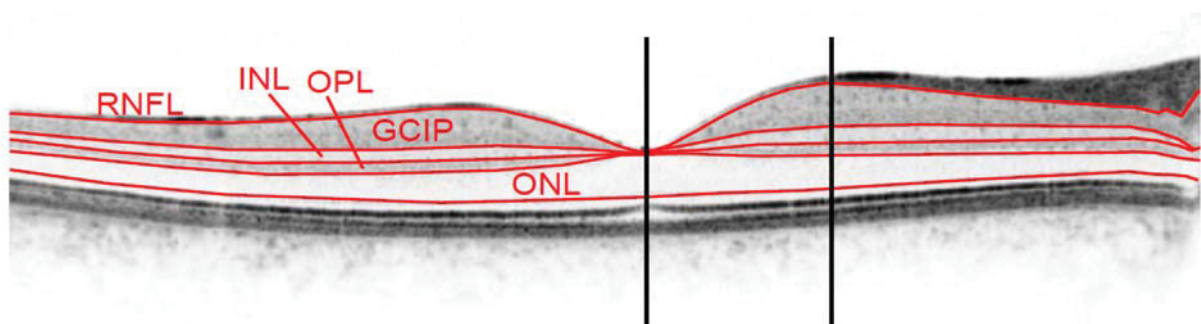


**Figure 14:** Assessment of the deeper retinal layers in ALS patients and controls. The deeper retinal layers were manually segmented in a single horizontal foveal scan (red lines). The thickness of the different layers was assessed 1. as mean thickness of the entire layers, 2. by a point estimate method (vertical black lines). RNFL= retinal nerve fiber layer; GCIP = ganglion cell/inner plexiform layer complex; INL = inner nuclear layer; OPL = outer plexiform layer; ONL = outer nuclear layer (from [Ringelstein et al. 2014b]; see above publication No. 4).

### Reduction of the mean RNFL and total macular thickness in ALS patients

The mean RNFL was significantly reduced in ALS patients by 6.7% (ALS  $93.2 \pm 10.7 \mu\text{m}$  vs. controls  $100.0 \pm 10.9 \mu\text{m}$ ;  $p=0.031$  GEE; Figure 15). The total macular thickness was significantly thinner as well by 2.6%, albeit less prominent (ALS  $309.8 \pm 17.3 \mu\text{m}$  vs. controls  $318.2 \pm 15.7 \mu\text{m}$ ,  $p=0.037$ ).

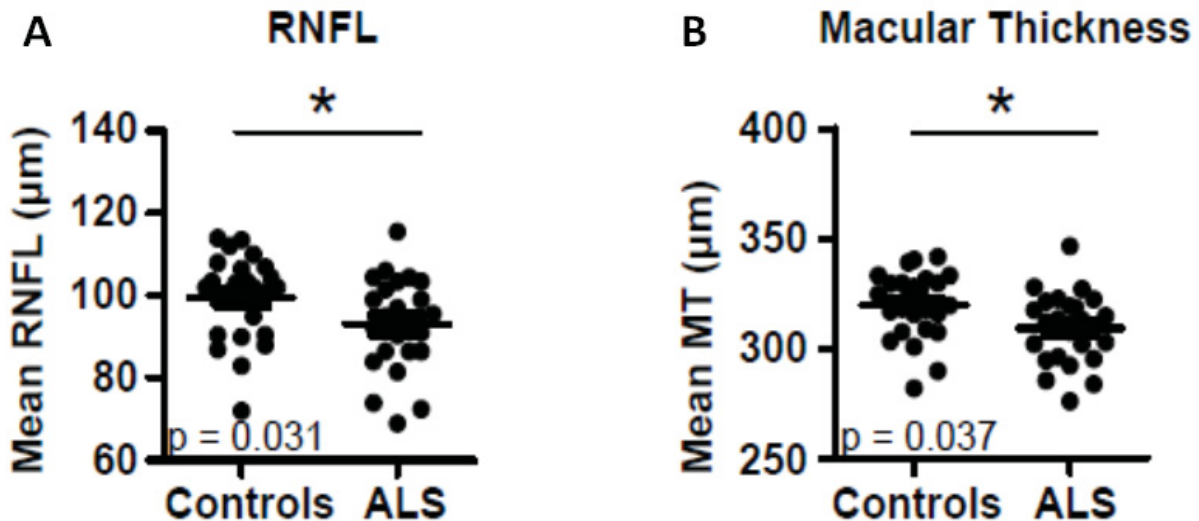


**Figure 15:** OCT results of the mean RNFL and Macular Thickness in ALS. Scatter plots display a significant (\*) reduction of the retinal nerve fiber layer (RNFL;  $p=0.031$ ; A) and the mean total macular thickness (MT;  $p=0.037$ ; B) in patients with ALS, compared to healthy controls. Each point represents the mean of the two eyes of one patient. The mean of all patients is indicated by a horizontal bar (from [Ringelstein et al. 2014b]; see above publication No. 4).

### OCT evaluation of the deeper retinal layers

Retinal segmentation revealed a significant reduction of the INL in ALS patients, ranging from -11.3% (mean thickness approach;  $p=0.001$ ) to -13.6% (P.E. approach;  $p<0.001$ ; Figure 16). No differences were observed for the mean retinal GCIP complex and the ONL. Of note, the OPL was thicker in ALS patients when analyzed as point estimates ( $p=0.001$ ).

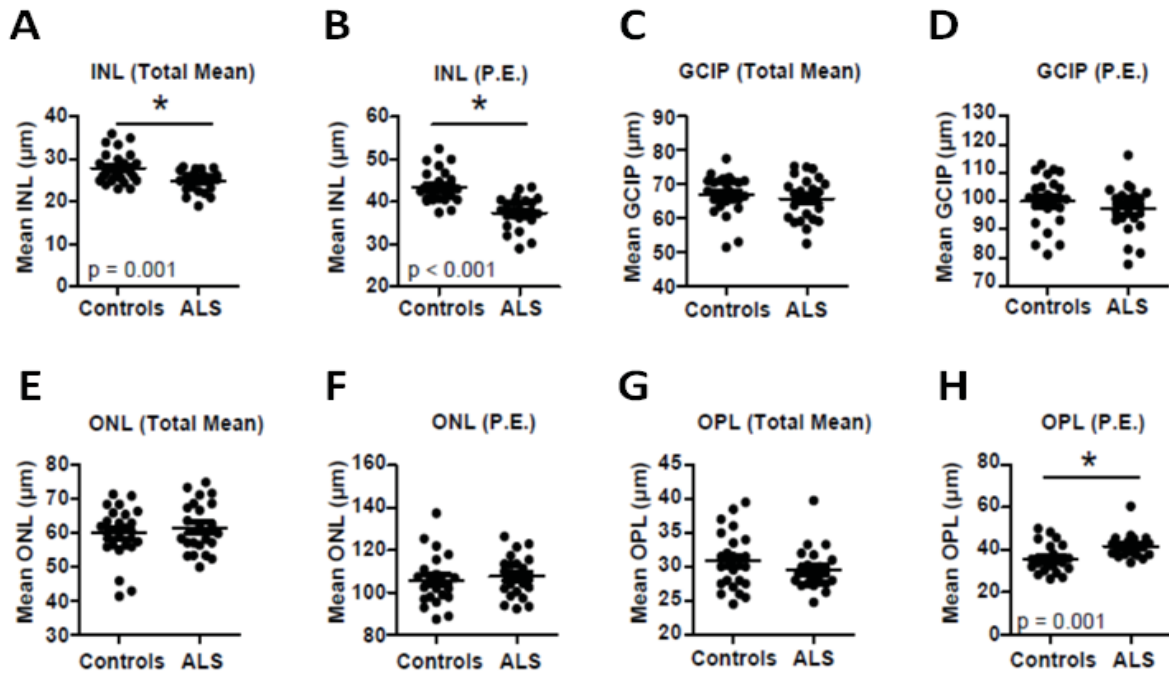


**Figure 16:** OCT results of the deeper retinal layers in ALS patients and controls. The INL was significantly (\*) reduced with both segmentation methods (mean thickness:  $p=0.001$  and P.E.:  $p<0.001$ ) compared to controls (A+B). No significant differences in the thicknesses of the GCIP (C+D) and the ONL (E+F) were detectable. The OPL was thicker in ALS patients, only when measured with the P.E. approach (G+H). Each point represents the mean of the two eyes of one patient. The mean of all patients is indicated by a horizontal bar. ALS = amyotrophic lateral sclerosis, GCIP = ganglion cell/inner plexiform layer complex, INL = inner nuclear layer, ONL = outer nuclear layer, OPL = outer plexiform layer, P.E. = point estimate (modified from [Ringelstein et al. 2014b]; see above publication No. 4).

### *Retinal parameters and clinical presentation*

Regarding the proportion of ALS patients with OCT alterations, we applied a cut-off of two standard deviations below the mean of normal controls to define abnormal values. We identified 3/24 (12.5%) ALS patients with abnormal RNFL thickness ( $<79.3 \mu\text{m}$ ), 3/24 (12.5%) cases with altered mean macular thickness ( $<289.6 \mu\text{m}$ ), 6/24 (25%) patients with reduced INL measured as point estimates ( $<35.8 \mu\text{m}$ ) and one patient (4%) with mean INL reduction ( $<20.49 \mu\text{m}$ ). Partial bivariate correlation analysis correcting for age and sex revealed no association of clinical disease characteristics (modified Rankin Scale) or disease duration with the thickness of the significantly altered RNFL, INL (measured as mean or P.E.) and total macula.

In conclusion, we here provided another morphological correlate for an extra-pyramidal, neuro-ophthalmological involvement in ALS patients, indicated by mild reductions of the total macular thickness and the RNFL axons, as well as a marked thinning of the cell bodies and nuclei of the horizontal, bipolar, and amacrine cells within the INL. Remarkably, the GCIP layer complex, situated between the RNFL and INL was not involved. Possibly the thinning of the RNFL is associated with degeneration of the corresponding neurons in the GCL but compensatory processes in the IPL mask the thinning of the GCL, when measuring the GCIP as a single entity. As distinct pathologies of the optic nerve have not yet been reported in ALS, and the fact that the RNFL but not the GCIP was significantly altered in this study, render a retrograde trans-synaptic degeneration rather improbable, even though voxel-based MRI volumetry and histopathology revealed occipital cortex affections of the brain [Brettschneider et al. 2013; Bede et al. 2012]. Therefore, in ALS one may assume a primary retinal process involving neuronal and consecutive axonal degeneration similar to the established mechanisms leading to upper and lower motor neuron degeneration.

This was the first SD-OCT study that could substantiate subtle retinal alterations in ALS, as a previous OCT report had failed to detect any retinal involvement [Roth et al. 2013]. Possibly the heterogeneity of the patient cohorts (definite ALS: 19.7% in their report vs. 83.3% in our work), the lack of gender-matching in the previous study and methodological differences (automated segmentation without manual correction vs. two different manual segmentation methods in this study) may have caused these diverging results. Nevertheless, our data support previously reported independent clinical and neurophysiological reports on visual disturbances in ALS and indicate a neurodegenerative process comprising the retina.

## **8. Susac Syndrome**

Susac syndrome (SuS), first described by John O. Susac in 1979 [Susac et al. 1979] is considered to be a rare autoimmune mediated micro-angiopathy leading to microvessel occlusions in the brain, inner ear, and retina [Dörr et al. 2013a; Dörr et al. 2014]. The prevalence of SuS is unknown as only slightly more than 300 individual cases with an estimated mean age at onset of 31.6 years and a female preponderance

of 3.5:1 have been published worldwide from our group until 2013 [Dörr et al. 2013b]. The characteristic clinical triad comprises encephalopathic and/or focal CNS dysfunction, sensorineural hearing disturbances and visual dysfunction [Dörr et al. 2014]. Cranial MRI shows multifocal, callosal accented T2-hyperintense “snowball lesions” in the acute phase, accompanied by distinct fiber disruption and substantial atrophy of the corpus callosum in advanced imaging techniques on the longer run [Susac et al. 2003; Kleffner et al. 2008; Wuerfel et al. 2012]. In the acute state, retinal fluorescein angiography (FA) depicts disease-specific branch retinal artery occlusions (BRAOs) and/or arterial wall hyperfluorescence (AWH), reflecting the impaired integrity of retinal endothelial cells [Egan et al. 2010; Dörr et al. 2014]. Relevant titers of antiendothelial cell antibodies have been observed in up to 25% of SuS patients, but their significance remains to be clarified [Jarius et al. 2014a]. Since only a small part of SuS patients presents with the characteristic symptom triad at disease onset and demographic (young female), clinical (focal neurological signs such as unilateral visual disturbance) and diagnostic findings (e.g. on brain MRI) may overlap, misdiagnoses with more common inflammatory CNS disorders, in particular with MS, often occur, which emphasizes the need for additional more specific, non-invasive diagnostic tools.

### **8.1. OCT in Susac syndrome**

Using TD-OCT, we could demonstrate patchy reductions of the peripapillary RNFL and the TMV in SuS patients (n=9) compared to RRMS patients and healthy controls [Brandt et al. 2012a]. Following these findings, we subsequently used tissue segmentation features of SD-OCT in a larger SuS patient cohort in order to analyze the involvement of distinct deeper retinal layers in comparison to RRMS eyes and to establish a link to vessel-related changes ([Ringelstein et al. 2015a]; see above publication No. 8).

Seventeen consecutive patients with SuS fulfilling the characteristic clinical triad, as well as seventeen age- and sex-matched patients with RRMS and seventeen age- and sex-matched HCs were enrolled in this multicenter study at the neurological Departments in Düsseldorf, Essen, Münster, and Berlin. All SuS patients had suffered at least once from a BRAO or AWH before study enrollment. Of 34 RRMS eyes, 9 eyes (of 7 patients) had a clinically defined history of optic neuritis (HON), whereas 25 eyes (of 15 patients) had no ON (noHON) prior to the OCT measurement.

Besides the mean pRNFL (12° peripapillary ring scan) and TMV (61 vertical volumetric B-scans), the thickness of the perifoveal mRNFL and the deeper retinal layers was semi-automatically assessed. Therefore, all 61 B-scans were *automatically* segmented by newest provided software from Heidelberg Engineering (Version 1.7.1.0), (Figure 4, see above). A post hoc *manual* correction was conducted for all three cohorts, performed by two independent raters for the SuS patients to assess the inter-rater reliability. In addition, among other ophthalmologic investigations, a 30° threshold automated perimetry to assess the visual field and a FA were performed in 14/17 and in 15/17 SuS patients, respectively.

Because the retinae of the SuS patients displayed scattered areas with obvious pathology within otherwise normal appearing tissue, the volume scans were divided into 8x8 squares (Figure 17), and the distribution of the thickness in the different squares was compared between SuS and RRMS patients and HC. Since the OPL showed the most striking reductions in SuS patients and the least thickness variations in MS patients and HC, the OPL thickness was used to differentiate between *pathological* and *normal appearing* retinal sectors of SuS patients, using an arbitrary cutoff value of <18 μm.

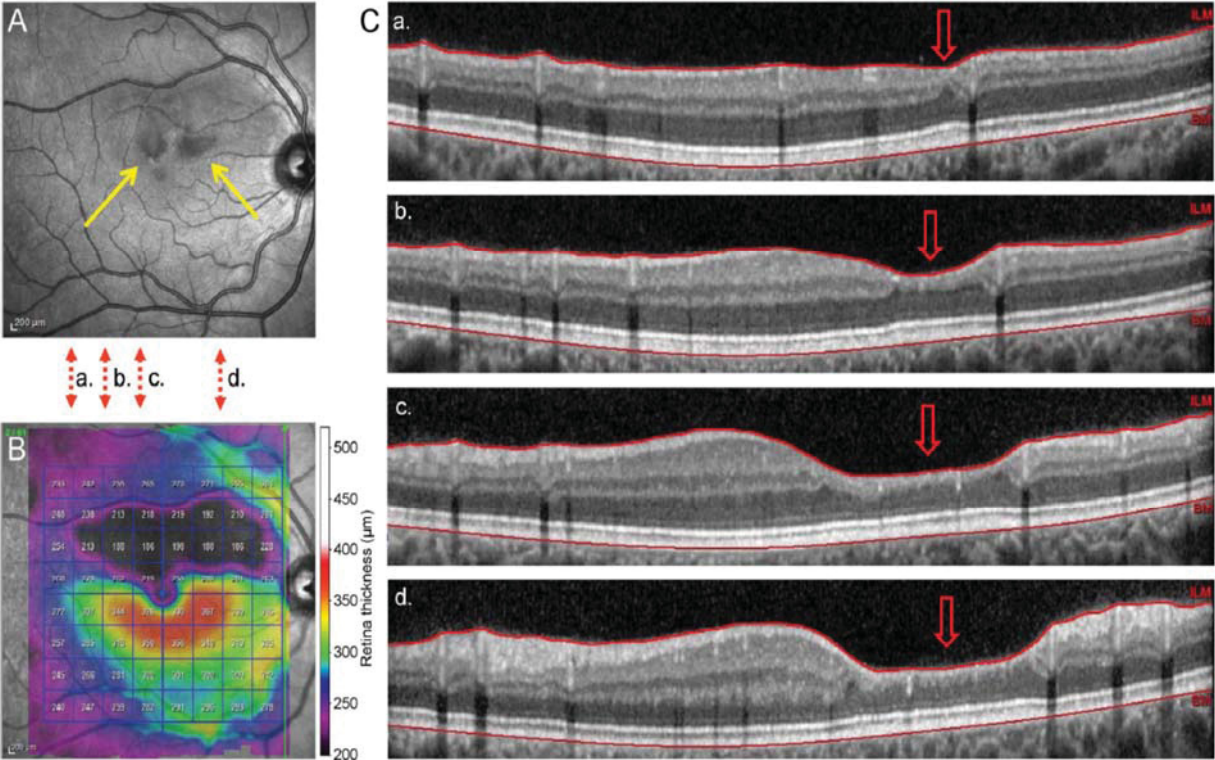


**Figure 17:** *Serious damage of the deeper retinal layers in a SuS patient.* Illustrative funduscopy example of a patchy area with obvious pathology (yellow arrows) between normal appearing tissue in an OCT scan of a SuS patient (A). In a color-coded thickness map derived from the volume data, generated by 61 vertical B-scans, the damaged area appeared much larger than suggested by the fundus image (B). Out of the 61 vertical scans, 4 examples (a.-d.) were extracted, evolving into cross-sectional images, and highlighting the serious damage of the inner retinal layers in distinct areas (C, open red arrows). ILM = inner limiting membrane, BM = Bruch’s membrane (from [Ringelstein et al. 2015a]; see above publication No. 8).

*Mean peripapillary RNFL and total macular volume*

The mean pRNFL and TMV were significantly thinner in SuS patients compared to HC ( $p < 0.003$  for both, GEE with Bonferroni correction). Compared to RRMS noHON eyes, only the pRNFL ( $p < 0.003$ ) but not the TMV ( $p = 0.219$ ) was thinner in SuS patients. Compared to RRMS HON eyes neither the pRNFL, nor the TMV ( $p > 0.99$  for both), differed significantly in SuS patients (Figure 18).

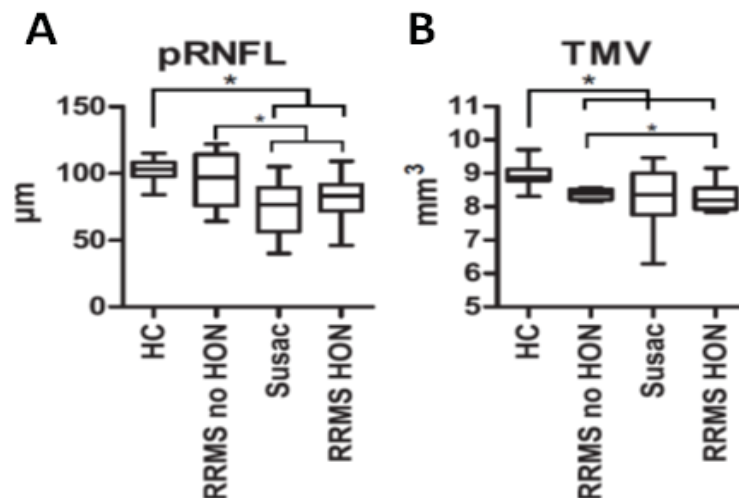


**Figure 18:** *Peripapillary RNFL and total macular volume measured with SD-OCT in patients with SuS, RRMS and HCs.* The mean peripapillary retinal nerve fiber layer (pRNFL) and the total macular volume (TMV) were significantly reduced in SuS patients compared to age- and sex-matched HCs ( $p < 0.003$  [\*] each; A+B). Compared to eyes of relapsing-remitting MS (RRMS) patients without a history of optic neuritis (no HON), only the pRNFL ( $p < 0.003$  [\*]) but not the TMV ( $p = 0.219$ ) was significantly thinner in SuS patients. Compared to RRMS eyes with a previous HON neither the pRNFL nor the TMV ( $p > 0.99$ , each) differed significantly in SuS patients (modified from [Ringelstein et al. 2015a]; see above publication No. 8).

### *Pathological and 'unaffected' sectors*

Using the cutoff of  $<18 \mu\text{m}$  OPL-thickness to define SuS pathological sectors, 16.5% of all analyzed retinal squares in SuS patient eyes but none of the sectors in RRMS and HC eyes fell below this threshold. Pathological squares were detectable in 23/34 (68%) SuS eyes (median: 16 affected sectors per eye, range 1-48) and occurred bilaterally in 11 patients and unilaterally in one. 11/34 (32%) eyes of 6 SuS patients (5 bilateral, 1 unilateral) did not reveal any severe retinal damage. Defining patients with at least one pathological sector in one eye as "positive", we were able to discriminate SuS patients with a sensitivity of 71% and a specificity of 100% from HCs and RRMS patients. Obvious pathological changes were mainly distributed to the temporal sector, where 29% of the squares revealed pathological findings (OPL  $<18 \mu\text{m}$ ); in the superior, inferior, central and nasal sectors the corresponding frequencies were 22%, 16%, 10%, and 8%, respectively.

### *Inner retinal layers*

In the *pathological* sectors of SuS eyes, a reduction of the mRNFL, GCL, IPL, INL, and OPL compared to RRMS eyes with and without a previous ON as well as compared to HC eyes was measured ( $p < 0.003$  for SuS vs. all 3 groups). By contrast, we did not find differences of the ONL and photoreceptor layers (PRL;  $p > 0.5$  for both) in comparison to both RRMS cohorts and HC (Figure 19).

In SuS retinal sectors *without* obvious pathology, the mRNFL and IPL were reduced compared to HC ( $p < 0.003$  for both), but only the IPL was thinner in comparison to corresponding sectors in RRMS noHON eyes ( $p = 0.008$ ). The mRNFL ( $p = 0.024$ ) and GCL ( $p = 0.032$ ) were thinner in RRMS HON eyes compared to unaffected SuS eyes (GEE analysis with post-hoc Bonferroni correction).

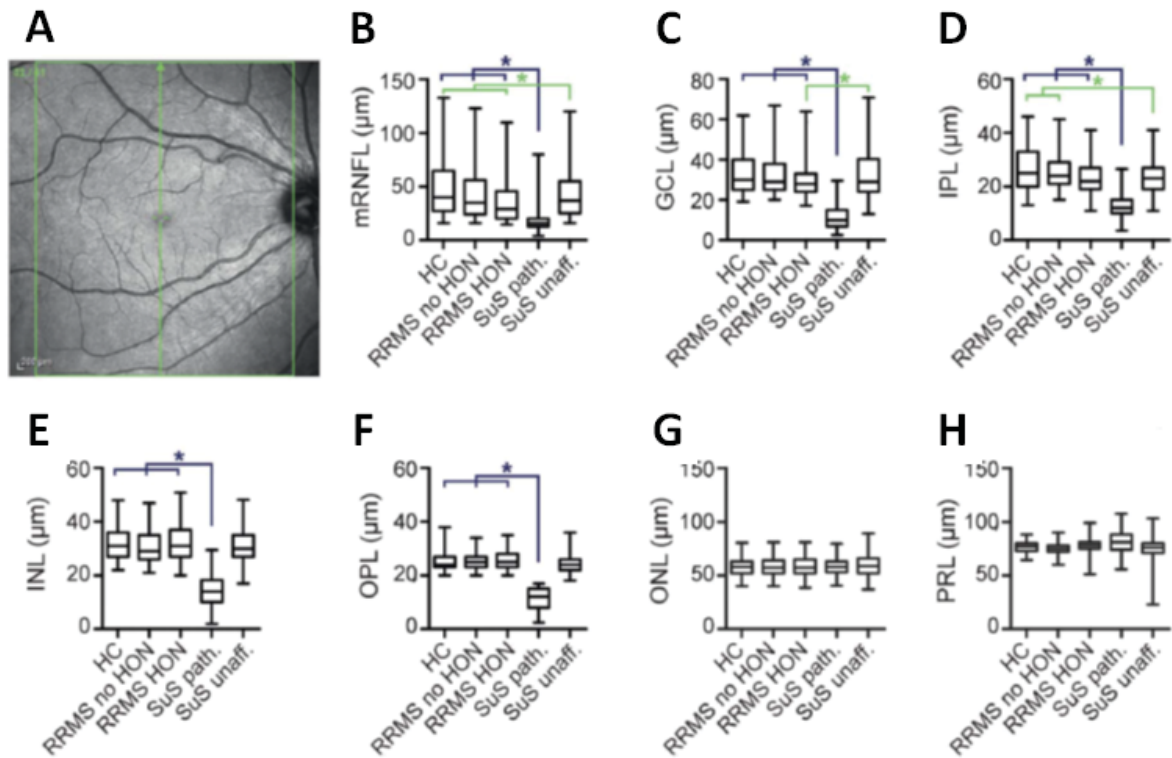


**Figure 19:** Inner retinal layer segmentation measured with SD-OCT in patients with Susac Syndrome, relapsing-remitting MS and healthy controls. After semi-automatic segmentation of 61 vertical B-scans (example in A) in sectors defined as pathological (SuS path.) the mRNFL, GCL, IPL, INL, and OPL were significantly reduced compared to healthy control (HC) and relapsing-remitting multiple sclerosis (RRMS) eyes with and without a history of optic neuritis (HON;  $p < 0.003$  [blue asterisk \*] for all layers; B-F). The ONL ( $p > 0.9$ ) and the PRL ( $p > 0.5$ ) were not altered compared to HC and RRMS patients either with or without HON (G+H). In SuS retinal sectors *without* obvious pathology (SuS unaff.), the mRNFL and IPL were significantly reduced compared to HC (both  $p = < 0.003$  [green asterisk \*], B+D), but this was true only for the IPL compared to corresponding sectors in RRMS patient eyes with no HON ( $p = 0.008$  [\*], D). The mRNFL ( $p = 0.024$ ) and the GCL ( $p = 0.032$ ) were thinner in RRMS eyes with HON compared to SuS eyes without obvious retinal pathology (B+C, green asterisk \*). mRNFL = macular retinal nerve fiber layer, GCL = ganglion cell layer, IPL = inner plexiform layer, INL = inner nuclear layer, OPL = outer plexiform layer, ONL = outer nuclear layer, PRL = photoreceptor layers (modified from [Ringelstein et al. 2015a]; see above publication No. 8).

#### Visual acuity and retinal fluorescein angiography

The mean visual acuity of SuS patients measured with ETDRS charts as logarithm of the minimum angle of resolution (logMAR) was normal with  $-0.033 \pm 0.102$  (right eyes)

and  $-0.041 \pm 0.107$  (left eyes). Retinal FA, performed in 15/17 (88%) SuS patients at the time of OCT investigation, revealed only one BRAO in one left temporal eye without evidence for any retinal damage in that area detectable by SD-OCT. Further vascular abnormalities, particularly in areas with severe OCT impairment, were not evident. Obviously they had already resolved over time.

#### *Associations between clinical measures and retinal pathology in SuS patients*

GEE-based regression analyses revealed no associations between disease duration or visual acuity and any of the retinal OCT parameters altered in SuS patients. To investigate the association of the deeper retinal layers with the 30° perimetries we divided the 64-square grid into four quadrants (nasal-superior, nasal-inferior, temporal-superior and temporal-inferior) with 16 squares each and correlated the mean thickness of the different layers with the opposite mean perimetry value (e.g. the nasal-superior OCT quadrant with the temporal-inferior perimetry quadrant). Visual field data of 9/14 evaluable SuS patient perimetries were associated with the thickness of the GCL and IPL ( $p=0.002$ ), INL ( $p=0.02$ ) and OPL ( $p=0.01$ ), whereas no associations were observed for the RNFL and ONL.

In summary, SD-OCT data on patchy pRNFL and TMV reduction in SuS as compared to RRMS and HC confirmed our previous TD-OCT results [Brandt et al. 2012b] albeit differences between SuS and RRMS patients with HON did not reach statistical significance, suggesting that these measures alone are not robust enough to clearly differentiate between SuS and MS. The here used approach to dichotomize between “unaffected” and “pathological” tissue squares revealed that in 68% of SuS patient eyes at least one retinal square was impaired and that the presence of at least one pathological square in either eye discriminated SuS from HC and RRMS with a sensitivity of 71% and a specificity of 100%.

The significant scattered reduction of virtually all inner layers sparing only the ONL and PRL in “pathological” retinal areas of SuS eyes compared to HCs and both RRMS groups, indicates the devastating and vascular-related tissue damage in SuS eyes compared to a milder and more diffuse inflammatory retinal degeneration in MS. Moreover, these findings correspond to the dualistic blood supply of the retina as the

layers affected are supplied solely by retinal circulation, whereas the undamaged ONL and PRL are supplied mainly by choroidal arteries [Kolb 1995].

Furthermore, the fairly disease-specific BRAOs and AWHs are important findings in SuS but usually resolve and are then no longer detectable by FA [Egan et al. 2014]. FA is an invasive procedure with possible side effects and does not allow for the evaluation of the retinal tissue itself. Thus, while FA can be considered as ophthalmologic diagnostic gold standard in the acute phase of SuS, its diagnostic value is rather modest in the inactive remission phase. OCT in contrast, captures the permanent scar-like tissue damage, which is obviously still present during later or inactive disease stages and, as shown by the association of the GCL, IPL, INL and OPL with the perimetry data, impacts the patients' visual function.

In conclusion, SD-OCT reveals characteristic retinal pathologies in SuS patient eyes, highlighting the retinal as opposed to a choroidal vascular pathogenesis of the disease and clearly delineates SuS from MS, as most important neurological differential diagnosis. Moreover, depicting permanent retinal tissue damage, associated with visual field defects, OCT provides complementary diagnostic information to FA in particular in later and chronic disease stages, when there may be no more BRAO or AWH detectable by FA. As OCT is a non-invasive, safe, and highly precise diagnostic tool, we expect an increasing impact of OCT on the future diagnostic workup of SuS.

## **9. Neuromyelitis Optica**

Neuromyelitis Optica (NMO, Devic's syndrome) is a rare (estimated prevalence < 1/10.000 inhabitants) inflammatory, autoimmune disease of the CNS characterized by relapsing ON and longitudinally extensive transverse myelitis (LETM) with frequently poor recovery [Ringelstein et al. 2010; Jarius et al. 2012b; Wingerchuk and Weinshenker2014]. NMO follows a relapsing-remitting course in 90 % of the cases with a marked female preponderance of 9:1 [Wingerchuk et al. 1999]. Usually, clinical history and presentation, MRI findings as well as CSF and serological tests guide the diagnostic work-up of NMO, particularly after the discovery of the NMO-IgG [Trebst et al. 2011a; Jarius et al. 2011; Jarius et al. 2012b]. This highly disease-specific serum autoantibody against aquaporin-4 (AQP4), a water channel present on astrocytic end

feet, proved NMO a new nosological entity and turned out to be extremely helpful in differentiating NMO from other demyelinating diseases, in particular MS (Figure 20) [Lennon et al. 2004 + 2005; Jarius et al. 2012a; Jarius et al. 2014b].

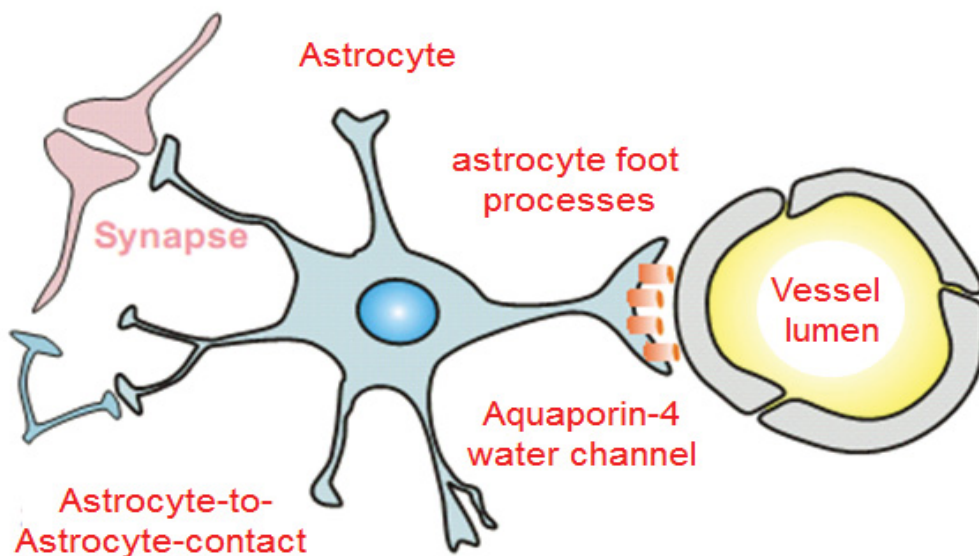


**Figure 20:** Cellular localization of the Aquaporin-4 water channel. The highly disease-specific autoantibody in Neuromyelitis Optica (NMO) is directed against aquaporin-4, a water channel present on astrocytic end feet with close contact to the abluminal part of brain vessels (modified from [Ringelstein et al. 2010]).

According to the 2006 revised NMO diagnostic criteria, applied also to our here mentioned studies, the diagnosis is based on both „absolute criteria“ (1. Optic neuritis, 2. Acute Myelitis) and at least 2 out of 3 „supporting criteria“ (1. Brain MRI not meeting the diagnostic „Barkhof criteria“ of MS, 2. LETM = contiguous spinal cord MRI lesion extending over at least three vertebral segments, 3. Positive NMO-IgG antibody detection in serum) [Wingerchuk et al. 2006]. However, using the AQP4-antibody (AQP4-Ab) as specific biomarker, it became obvious in recent years that the clinical variety of NMO is much more heterogeneous than reflected by the 2006 diagnostic criteria. Hence, so called NMO spectrum disorders (NMOSD) can be defined in patients with AQP4-Ab seropositivity and isolated (recurrent) LETMs or ONs, brainstem syndromes involving the area postrema, diencephalic symptoms, or clinical signs related to lesions in periependymal regions [Wingerchuk et al. 2007; Ringelstein et al. 2014a]. In consequence, these findings necessitated a revision of diagnostic criteria for NMOSD that was published in July 2015 [Wingerchuk et al. 2015].

Because clinical and diagnostic findings in NMO may strongly overlap with those in MS, the most important differential diagnosis, and AQP4-Abs are detectable only in up to 80% of NMOSD patients, establishing the correct diagnosis can still be challenging. Furthermore, LETM is not pathognomonic for NMOSD, as longitudinally extensive spinal cord lesions (LESCLs) can also be observed with coexisting systemic autoimmune diseases, infections, vascular and metabolic disorders or may mimic intramedullary tumors or paraneoplastic myelopathies [Trebst et al. 2011b; Kitley et al. 2012; Ringelstein et al. 2014a].

### **9.1. Contribution of spinal cord biopsies to the diagnosis of NMOSD**

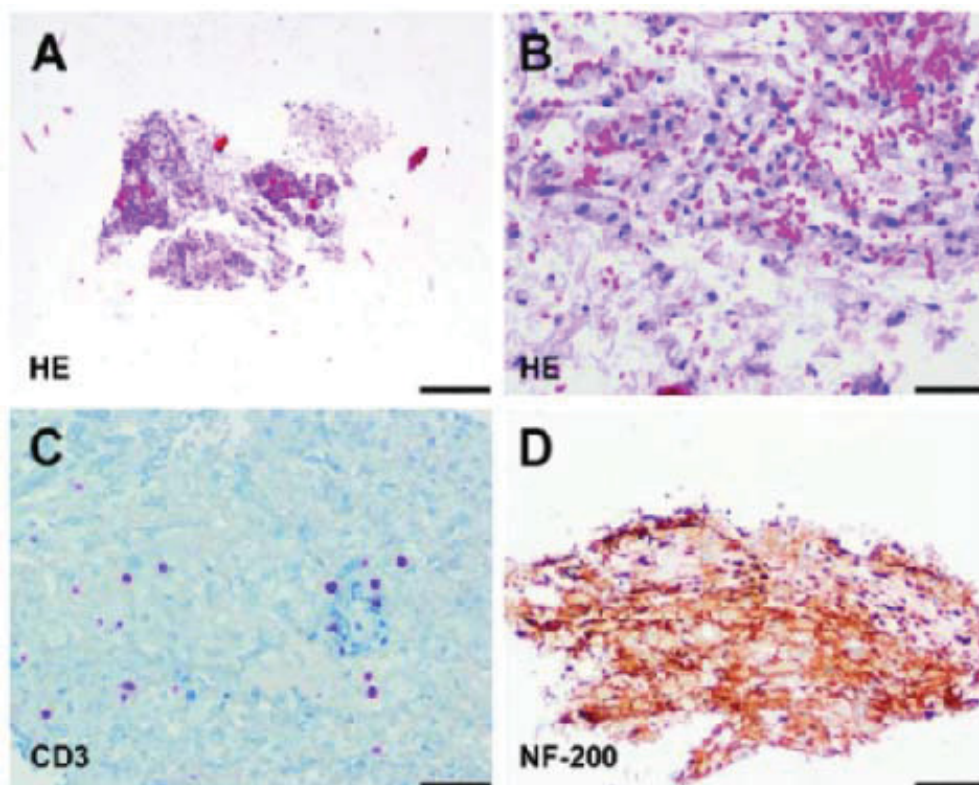
In this study, we aimed to determine the diagnostic value of spinal cord biopsies performed in patients, who presented with LESCLs of unknown etiology during some point of their disease course, and turned out postoperatively to suffer from AQP4-Ab seropositive NMOSD. Out of the total cohort of 175 NMOSD patients at that time captured by the German Neuromyelitis Optica Study Group ([www.nemos-net.de](http://www.nemos-net.de)), we identified seven female NMOSD patients, who underwent such spinal cord biopsy ([Ringelstein et al. 2014d]; see above publication No. 5). Fortunately, we were able to perform a neuropathological reevaluation in 4 out of these 7 cases, using the original biopsy specimens.

The patients' median age was 40 years (range 24–52) at first clinical presentation and 43 years (range 29–57) at the time of biopsy. The LESCL was the initial manifestation in four patients, whereas three patients had experienced an inflammatory episode suggestive of NMOSD prior to biopsy (ON or rhombencephalitis). Suspected diagnoses leading to biopsy included 'astrocytoma', 'atypical pen-like glioma', 'tumor of unknown etiology', 'spinal tumor' and 'intramedullary tumor'. Spinal MRI showed non-homogeneous gadolinium enhancement in 6/7 patients with pronounced myelon swelling between the medulla oblongata and Th9 (range), extending over more than 6 segments (mean, range 4–15). Brain MRIs prior to biopsy were normal in 4/7 patients or revealed unspecific white matter lesions in 3/7 cases. CSF analysis showed a mild (5/7 patients) or moderate pleocytosis (2/7 patients) and isolated oligoclonal bands in one patient.

Remarkably, initial histopathological diagnoses did not suggest an NMO-related process but were reported as (a) 'inflammatory destructive lesion', (b) 'glial tumor with

desmoplastic and angiogenic compound of low malignancy', (c) 'angiodysgenetic necrotizing myelopathy Foix-Alajouanine', (d) 'subacute necrosis, no tumor', (e) 'tumor-free spinal cord', (f) 'CNS tissue with severe reactive and resorptive changes, no neoplasia' and (g) 'reactive CNS tissue with inflammation and resorptive changes'. NMO histopathology in general is characterized by inflammatory, often destructive, demyelinating lesions with perivascular IgG and complement deposition, hyalinized vessels and eosinophilic granulocytes. An astrocytic pathology with AQP4 loss extending beyond the area of demyelination is typical and oligodendrocytes may be lost within lesions [Lucchinetti et al. 2002; Misu et al. 2007].

Re-evaluation of the four available spinal biopsies was limited by the small sample size and numbers of sections. Demyelination was evident in all cases. Inflammation (CD3), extensive axonal damage (Bielschowsky silver impregnation) and hyalinized vessels were evident in 3/3 biopsies. Perivascular complement depositions were not found (0/3; C9neo) and complement within macrophages was evident in one case (1/3; C9neo). Only in one biopsy were eosinophilic granulocytes present. Both of the two cases in which Glial fibrillary acidic protein (GFAP) and AQP4 could be stained showed astrocytic dystrophy and loss, as well as loss of AQP4. Oligodendrocytes (NOGO-A or CNPase staining) were depleted in 2/2 biopsies (Figure 21).



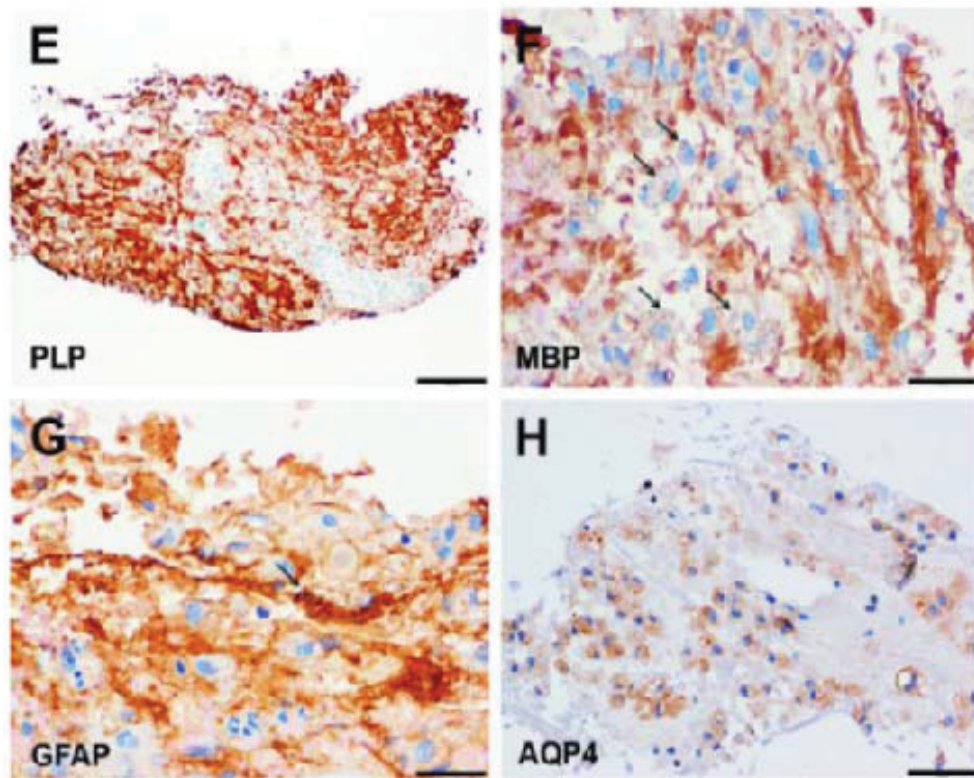


**Figure 21: Histology of spinal cord NMO lesion.** Shown here is a destructive inflammatory demyelinating lesion with AQP4 loss. A small specimen is available for analysis from an eloquent lesion location within the spinal cord (A; HE). Higher magnification shows a destructive, loose-textured lesion with numerous macrophages (B; HE) and a T cell infiltrate (C; anti-CD3). Only few axons are preserved, underlining the destructive nature of the lesion (D; anti-NF200). Although the myelin is partially preserved (E; anti-PLP), higher magnification clearly shows myelin degradation products within macrophages, indicating active demyelination (F; anti-MBP; arrows indicate macrophages with myelin debris). Astrocytes appear partially dystrophic and partially depleted (G; anti-GFAP; arrow indicates dystrophic astrocyte), whereas AQP4 staining of astrocytes is completely lost (H; anti-AQP4). Macrophages show AQP4-positive degradation products within their cytoplasm (H; brown-colored macrophages). Scale bars: A: 500  $\mu\text{m}$ ; B-D: 100  $\mu\text{m}$ ; E: 200  $\mu\text{m}$ ; F+G: 50  $\mu\text{m}$ ; H: 100  $\mu\text{m}$  (from [Ringelstein et al. 2014d]; see above publication No. 5).

All patients were AQP4-Ab seropositive, when tested after the spinal biopsy using cell-based assays. The final diagnoses were NMO (4/7) and NMOSD-related LETM (3/7) at an average of 68.4 months (range 0.5–160) after initial symptoms and 30.3 months (range 0.25–103.5) after biopsy. Notably, three patients were biopsied before AQP4-

Ab testing was routinely available (one in 1995, two in 2002) [Lennon et al. 2005]. Testing was available but not performed before surgery in all four other cases. The median EDSS prior to biopsy was 4.0 (range 2.5–8.0) and 8.0 (range 3.0–8.5) in the first few days thereafter, due to severe complications like CSF leakage, epidural hematoma (Figure 22), and postoperative spinal trauma in 5/7 patients. Biopsy-related deterioration persisted in 2/7 patients, with an elevated EDSS score of 7.5 (median; range 2.0–8.5) at last follow-up (mean 86.6 months after spinal biopsy; range 20–218).

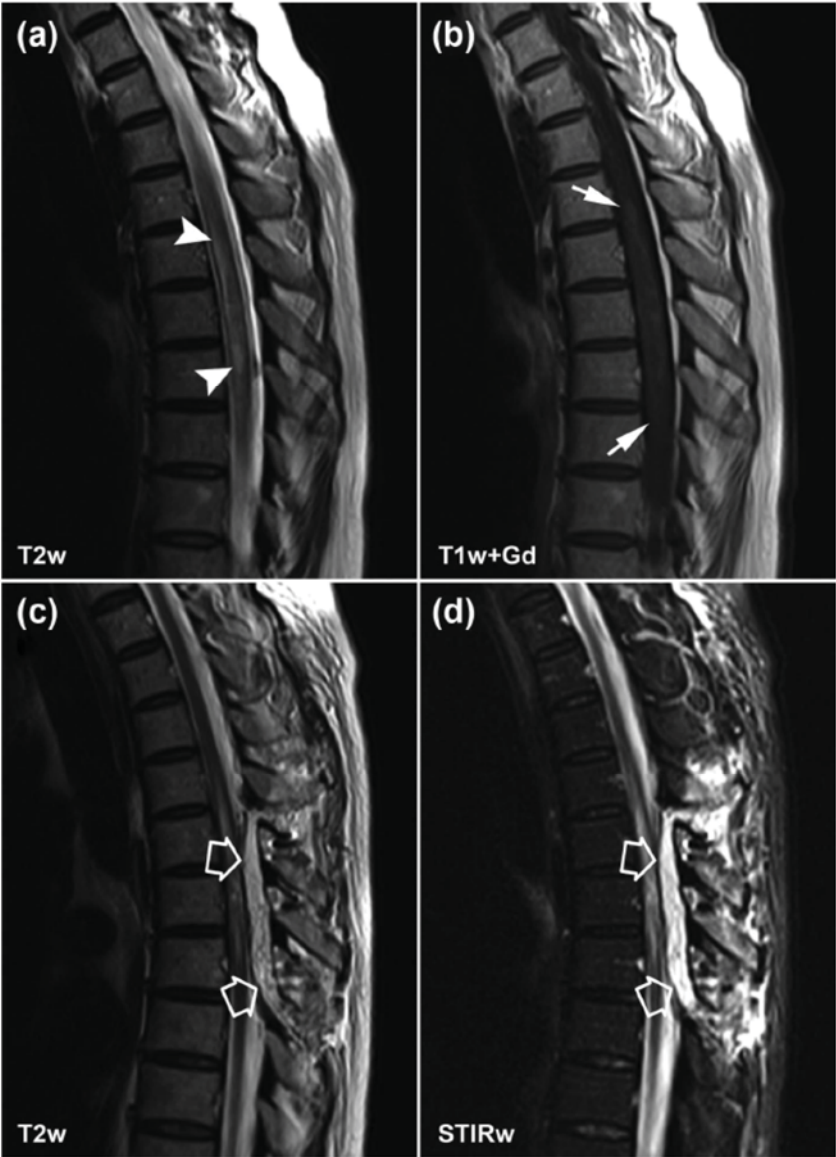


**Figure 22:** Pre- and postoperative spinal magnetic resonance imaging (MRI). A longitudinal and space-consuming transverse myelitis between vertebral segments Th2 and Th7 before diagnostic biopsy with a particular swelling of the spinal lesion in a T2-weighted image ((a), white arrow heads) and low contrast Gadolinium enhancement in a T1-weighted image ((b),

white arrows) is shown. (c) and (d) illustrate the postoperative state after spinal biopsy at level Th5. Epidural bleeding occurred at levels Th4–Th7 with ventral dislocation and compression of the myelon (open white arrows in T2-weighted- (c) and short T1 inverse recovery (STIR)-weighted- (d) images) (from [Ringelstein et al. 2014d]; see above publication No. 5).

In summary, a CNS biopsy undoubtedly represents the ultimate diagnostic step for evaluation of an unclear LESCL because it may have severe adverse effects, particularly in the inflamed spinal cord. Here, five patients experienced transient complications in the first few days after biopsy, leading to persistent, severe paraparesis in one patient and permanent tetraparesis with wheelchair dependence in another. Moreover, in this case series, initial routine histopathology excluded tumors in 6/7 patients, but did not lead to the correct diagnosis, as certain neuropathological findings typical of NMO like perivascular depositions of activated complement were not detectable. This observation is in line with previous reports suggesting heterogeneity of NMO lesions according to lesion stage and biopsy site [Lucchinetti et al. 2002; Misu, et al. 2007].

Taken all together, our findings emphasize the importance of AQP4-Ab testing for the diagnostic work-up of LESCL. Considering the possible adverse effects and sequelae of biopsy procedures, AQP4-Ab testing using assays with sufficient sensitivity and specificity [Waters et al. 2012] is mandatory in patients with inconclusive spinal cord lesions prior to biopsy. Biopsies of LESCLs should be avoided or limited to cases in which other tests only provide inconclusive diagnostic findings.

## **9.2. Visual evoked potentials in NMOSD**

As NMO primarily affects the spinal cord and the optic nerve, investigations of the functioning of the visual pathway are quite reasonable. In this context, easy-to-apply, reproducible, cost-efficient diagnostic tools like VEP, that can evaluate and quantify the impact of NMOSD-associated ON and possibly differentiate NMOSD from other CNS disorders like MS are highly desirable.

VEPs are an appropriate diagnostic tool to assess the visual pathway's conduction capacity from the retina to the occipital cortex and characteristically show prolonged P100 latencies but normal amplitudes in classical MS [Halliday et al. 1973; Matthews et al. 1977]. In contrast, in a small Afro-Brazilian cohort of 19 NMO patients (8 out of

them AQP4-Ab seropositive) VEPs revealed an absent response in 47.4% of eyes, as well as reduced amplitudes with normal P100 latencies in 34.2% of patient eyes, with the latter being defined as typical 'NMO pattern' by the authors [Neto et al. 2013]. In consequence, we analyzed VEPs in a larger and better defined cohort of predominantly Caucasian patients with NMO and AQP4-Ab positive NMOSD in comparison to HCs, to prove whether we could confirm the distinct VEP 'NMO pattern', that would help to differentiate between NMO and MS ([Ringelstein et al. 2014c]; see above publication No. 5).

We retrospectively analyzed full-field pattern-reversal VEP datasets from a large cohort of 43 patients with definite NMO according to the 2006 diagnostic criteria [Wingerchuk et al. 2006] and 18 additional patients with AQP4-Ab seropositive NMOSD [Wingerchuk et al. 2007] and compared them with 61 age- and sex-matched HC in a multicenter study in four German tertiary-referral neurological centers in Düsseldorf, Bochum, Berlin and Essen. VEPs were performed using full-field monocular stimulation with black and white checkerboards (12 mm/41 min), reversed at a rate of 1.5–2/s and were recorded in two trials for each eye, averaging > 150 responses, with electrodes positioned at Oz (active) and Fz (reference) sites. We measured peak latencies of N75, P100 and N140, and P100-N140 peak-to-peak-amplitudes. Cutoffs for normal values were < 120 ms for P100-peak latencies and  $\geq 3$   $\mu$ V for P100-N140 peak-to-peak-amplitudes. These cutoff limits were previously established by internal validation measurements and represent values beyond two standard deviations from the mean.

### *Patient characteristics*

We investigated 51 female and 10 male patients: 59 were of Caucasian origin, one African-American and one of Asian descent. The mean age at disease manifestation was  $36.8 \pm 14.9$  years and  $43.5 \pm 13.3$  years at the time of VEP measurement, and their EDSS was  $4.2 \pm 2.2$ . Anti-AQP4-Ab testing using cell-based assays [Jarius et al. 2010] was available in 59/61 patients (96.7%), with 50 cases (84.7%) being positive and nine (15.3%) negative. ON as a mandatory diagnostic criterion was diagnosed in all 43 NMO patients, but only in four of the 18 NMOSD patients (22.2%); the residual 14 (77.7%) AQP4-Ab-seropositive NMOSD patients presented with LETM (Table 2).

**Table 2: VEP parameters, demographic and clinical data of NMO and NMOSD patients and healthy controls.**

Parameters	Healthy controls		NMO		NMOSD		NMO+NMOSD		No history of ON		History of ON		AQP4-Ab-seronegative		AQP4-Ab-seropositive	
	Mean	SD	Mean	SD	Mean	SD	Mean	SD	Mean	SD	Mean	SD	Mean	SD	Mean	SD
Age (years)	43.5	12.9	43.8	12.4	42.8	15.8	43.5	13.3	41.8	13.7	44.9	12.9	42.0	10.8	44.1	13.8
EDSS	n.a.	n.a.	4.4	2.2	3.7	2.3	4.2	2.2	3.3	1.9	4.9	2.1	3.3	2.0	4.3	2.2
Disease duration (years)	n.a.	n.a.	6.8	5.9	4.1	6.5	6.0	6.1	4.9	5.8	7.0	6.4	6.0	6.6	5.7	5.8
N75 latency (ms)	74.1	4.5	<b>90.3***</b>	22.7	85.7	22.3	<b>89.1***</b>	22.6	82.6	17.9	<b>93.9***</b>	24.8	86.2	16.2	89.2	23.5
P100 latency (ms)	103.3	5.5	<b>126.2***</b>	21.0	<b>115.9*</b>	20.4	<b>122.9***</b>	21.3	<b>113.4**</b>	17.9	<b>131.2***</b>	20.7	<b>123.2***</b>	10.4	<b>122.6***</b>	22.7
N140 latency (ms)	138.8	11.9	<b>164.2***</b>	24.0	<b>158.2*</b>	27.9	<b>162.5***</b>	25.1	153.3	25.4	<b>170.0***</b>	22.7	163.1	14.8	162.3	26.5
Amplitude (µV)	9.2	5.0	<b>5.9***</b>	2.9	7.2	3.3	<b>6.3***</b>	3.1	7.7	3.0	<b>5.2***</b>	2.7	6.8	3.3	<b>6.3***</b>	3.1

Indicated are the means and standard deviations (SD) for the acquired VEP parameters (N75, P100, N140 latencies and amplitudes) for the total patient cohort (NMO+NMOSD), for NMO and NMOSD patients alone and healthy controls. Additionally, age, EDSS and disease duration at the time of VEP are presented (EDSS data available of 36 NMO and 11 NMOSD patients). Significant differences to healthy controls are indicated by asterisks (\*\*p<0.0001, \*\*\*p<0.001, \*p<0.05, GLM analysis for comparison of healthy controls with the combined NMO/NMOSD group and Kruskal-Wallis analysis of variance with Dunn's post hoc test for comparison of the three groups). AQP4-Ab: anti-AQP4 antibody, EDSS: Expanded Disability Status Scale, n.a.: not applicable, NMO: Neuromyelitis Optica, NMOSD: NMO spectrum disorder, ON: optic neuritis, VEP: visual evoked potential (modified from [Ringelstein et al. 2014c]; see above publication No. 5).

### General VEP responses

A VEP response was detectable in 74 of 86 (86.0%) NMO eyes and in 35 of 36 (97.2%) NMOSD eyes. Compared to healthy controls, N75, P100 and N140 latencies were significantly delayed and amplitudes were reduced in both the combined NMO/NMOSD ( $p < 0.0001$ ) and the NMO group. P100 and N140 latencies were also delayed in the NMOSD eyes alone (Figure 23). An analysis with respect to a previous history of ON (HON) revealed significantly prolonged P100 latencies in eyes both with and without HON, while N75 and N140 latencies were only significantly prolonged and their amplitudes reduced in the eyes with HON.

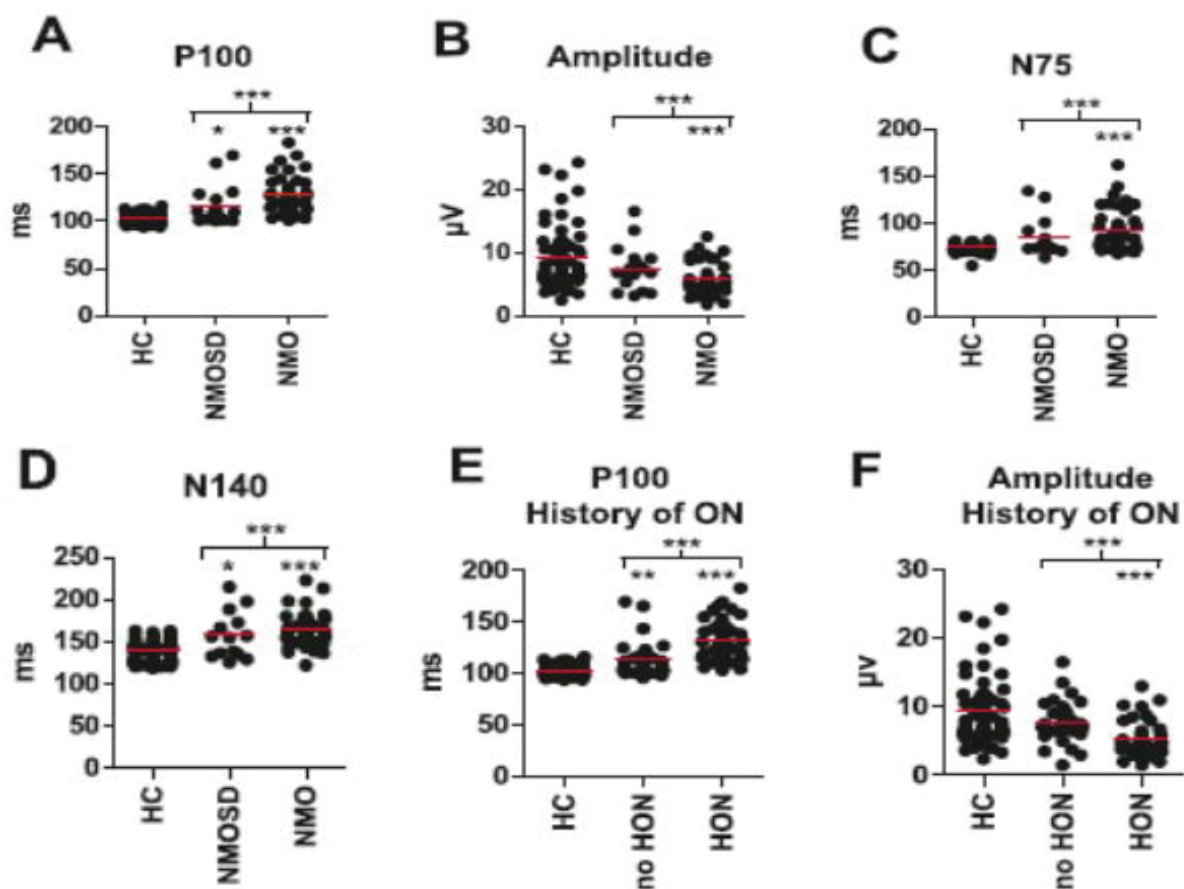


**Figure 23:** General VEP parameters in NMO/NMOSD and the impact of ON. Compared to healthy controls the P100 latency was significantly delayed in both, NMOSD and pure NMO patient eyes, whereas the P100-N140 amplitude was reduced only in the total NMOSD/NMO patient cohort (indicated by squared brackets) and in definite NMO patients (A+B). N75 latencies were prolonged only in the NMO group compared to HC (C), whereas N140 latencies were significantly delayed in NMO and NMOSD patients versus controls (D). Patient eyes with a previous history of optic neuritis and those without a prior ON revealed significantly prolonged

P100 latencies, whereas the amplitude was reduced only in HON patients compared to HC (E+F). Each point represents the mean of patients or HCs eyes, except for E and F, where eyes are separated according to the history of ON. Significant differences are indicated by asterisks (\*\* $p < 0.001$ , \* $p < 0.05$ ). HC: healthy control, NMO: Neuromyelitis Optica, NMOSD: NMO spectrum disorder, HON: history of optic neuritis (modified from [Ringelstein et al. 2014c]; see above publication No. 5).

### Impact of anti-AQP4 antibody serostatus

Analysis of the AQP4-Ab status revealed no differences in P100 latencies nor amplitudes between seropositive and -negative patients (Figure 24); however, P100 latencies were significantly prolonged in both the seropositive and -negative patients, compared to HCs, while the reduction of amplitudes compared to HCs was only significant for the seropositive patients. Visual acuity correlated negatively with P100 latencies and positively with amplitudes ( $p < 0.001$ ,  $r = -0.46$  and  $r = 0.48$ , respectively).

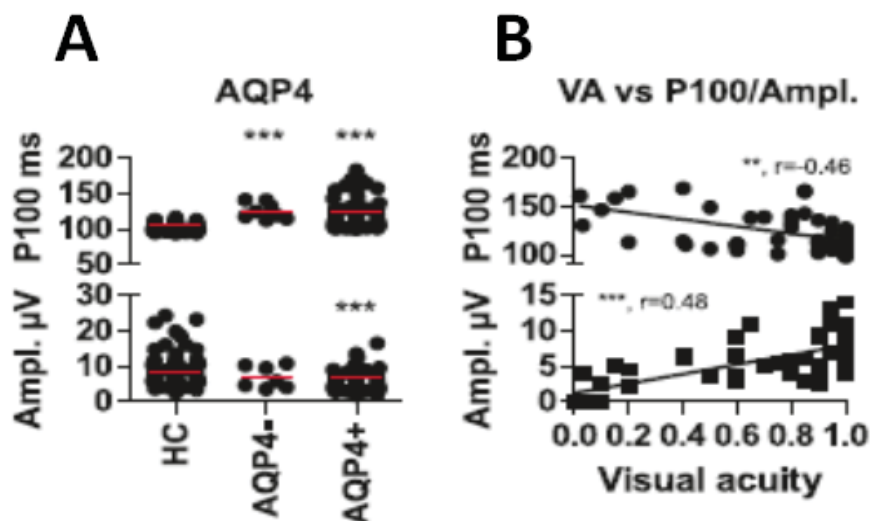


**Figure 24:** Impact of AQP4-Ab status on P100 latencies, amplitudes and visual acuity. P100 latencies were significantly increased in both, seropositive and -negative patients compared to healthy controls, while the amplitude reduction was only significant for seropositive patients (A). Visual acuity in the total patient cohort correlated negatively with P100-latencies and positively with amplitudes ( $r = -0.46$  and  $r = 0.48$ , respectively, B). Each point represents the mean of patients or HCs eyes. Significant differences are indicated by asterisks (\*\* $p < 0.001$ , \* $p < 0.05$ ). Ampl.: amplitude, AQP4-Ab: anti-AQP4 antibody, HC: healthy control, VA: visual acuity (modified from [Ringelstein et al. 2014c]; see above publication No. 5).

### *Investigation of a specific NMO pattern*

Of the NMO eyes generating responses, 36 out of 74 (48.6%) had prolonged P100 latencies ( $\geq 120$  ms) and 28 out of these 36 (which is 37.8% of 74) had normal amplitudes of  $\geq 3$   $\mu$ V. Reduced amplitudes were detectable in 10 of the 69 NMO eyes with stimulus response (14.5%; data not available for five eyes). Of the NMOSD eyes generating responses, 10 out of 35 (28.6%; four LETM and six ON eyes) had prolonged P100 latencies, and 9 out of these 10 (25.7% of 35) had normal amplitudes. Amplitude reduction was detectable in only 1 of 33 NMOSD eyes, in a patient with AQP4-Ab seropositive ON (3.0%; data not available for two eyes). Only one NMOSD and none of the NMO eyes fulfilled the proposed 'NMO pattern' with normal P100 latencies and reduced amplitudes, while 28 NMO and 9 NMOSD eyes (37/109; 33.9%) presented the typical MS pattern with prolonged latencies and normal amplitudes. No evoked response was generated in 12/86 (14.0%) NMO and 1/36 (2.8%) NMOSD eyes.

Taken together, our data demonstrates frequent latency prolongations in > 40% of NMO eyes and a less frequent occurrence of amplitude reductions, suggesting a mainly demyelinating affection of the visual pathway. We found these proportions to be similar to those observed in MS [Halliday et al. 1973; Matthews et al. 1977] in contrast to the specific 'NMO pattern' previously proposed by Neto and colleagues [Neto et al. 2013]. Interestingly, we noted delayed P100 responses, even in eyes without HON, suggesting subclinical involvement. The differences between the previous report from Brazil and our study could possibly be explained by different ethnic backgrounds (73.7% African-Brazilians vs. 96.7% Caucasians), or by the different AQP4-Ab status (21% seropositive NMO patients in their study vs. 84.7% in our cohort).

We conclude that in NMO patients of predominantly Caucasian origin, VEP latencies are often delayed, indicating a primarily demyelination of the optic pathway, even without a previous history of optic neuritis. A distinct VEP pattern in NMO patients, contrasting to what is known for MS, would help for differentiation of these two disease entities, but was not evident in our study.

### **9.3. Current treatment options in NMOSD**

As mentioned, NMO usually follows a relapsing-remitting disease course, often with devastating attacks, frequently leading to functional blindness or severe disability. Acute NMO attacks are treated with high dose steroids or require an escalation therapy with plasma exchange [Kleiter et al. 2015]. The risk of a second attack (ON or LETM) within 12 months after an initial LETM in AQP4-Ab seropositive patients is higher than 50% [Weinshenker et al. 2006]. Therefore, early and aggressive relapse prevention is of particular importance in NMOSD patients [Trebst et al. 2014].

As randomized-controlled studies are lacking to date, first line therapy recommendations are mainly based on expert opinions, retrospective cohort studies and smaller prospective case series. Against this background, for mild NMO cases, long-term immunosuppression with azathioprine [Elsone et al. 2014] or mycophenolate mofetil [Huh et al. 2014] has been recommended, with methotrexate being an alternative treatment option [Kitley et al. 2013]. In patients with more severe NMO courses, rituximab [Kim et al. 2013] and mitoxantrone [Kitley et al. 2011] have been reported to diminish relapse frequency. In this context, we reported an AQP4-Ab-seropositive NMO patient, who became pregnant during rituximab treatment, requiring the cessation of the medication. Low-dose rituximab (100 mg) restarted two days after delivery could, however, prevent the expected postpartum rebound NMO relapses [Ringelstein et al. 2013a].

Of note, in all the above mentioned retrospective case series, individual NMO patients stand out with persistent disease activity or suffering from major adverse events rendering additional potent and well tolerable medications desirable. Furthermore, we and others reported, that established MS therapies such as interferons, natalizumab or fingolimod show little if any efficacy, or are even detrimental in NMOSD patients [Min et al. 2012; Shimizu et al. 2010; Harmel et al. 2014; Kleiter et al. 2012].

### **9.4. Tocilizumab treatment in NMOSD**

In this context, we evaluated the therapeutic use of tocilizumab (TCZ), a humanized antibody targeting the Interleukin-6 (IL-6) receptor, in highly active NMOSD patients ([Ringelstein et al. 2015b]; see above publication No. 7). The aim of our retrospective multicenter study was to evaluate the long-term efficacy and safety of TCZ in

exclusively Caucasian NMOSD patients, who had not adequately responded to previous first- and second-line treatments.

TCZ has already been approved for the therapy of rheumatoid arthritis and systemic juvenile idiopathic arthritis, where increased serum IL-6 levels have been shown to promote synovitis and induce progressive bone resorption and cartilage degeneration [Hashizume et al. 2014]. IL-6 has also been characterized to mediate inflammation, demyelination, and astrogliosis in the CNS and is secreted primarily by activated astrocytes upon infection, stroke, and inflammation [Van Wagoner and Benveniste 1999]. In NMO patients, increased levels of IL-6 were detected in the CSF and serum, particularly in AQP4-ab seropositive patients with severe disease activity [Uzawa et al. 2010]. Using an ex vivo spinal cord organotypic slice model, NMO-IgG-mediated AQP4 loss and subsequent demyelination were markedly increased in the presence of IL-6 [Zhang et al. 2011]. Finally, IL-6 enhances survival and AQP4-ab synthesis of CD19<sup>int</sup>CD27<sup>high</sup>CD38<sup>high</sup>CD180<sup>-</sup> plasmablasts, which were shown to circulate at increased levels in the peripheral blood of NMO patients [Chihara et al. 2011].

In our study, eight Caucasian female patients with AQP4-Ab seropositive NMO (n=6) and NMOSD (n=2) were retrospectively analyzed at the Departments of Neurology in Düsseldorf, Bochum, Osnabrück and Wiesbaden. Before the start of TCZ, all patients had been pre-treated with immunomodulatory/immunosuppressant medications, including interferon (IFN)- $\beta$  1b (n=3 patients), IFN- $\beta$  1a (n=2), azathioprine (n=2), mitoxantrone (n=2), mycophenolate mofetil (n=1), natalizumab (n=1), glatiramer acetate (n=1), alemtuzumab (n=1), and monthly i.v. steroids (250mg/mo., n=1). Of note, the B-cell depleting antibody rituximab had been given at least once in every patient prior to TCZ (range 1-3 therapeutic cycles, comprising 1-2 infusions per cycle). TCZ was, for safety reasons, initiated in 4/8 patients with a reduced dosage of 6 mg/kg body weight in 4- to 6-week intervals and was switched to 8 mg/kg in 2 of these 4 patients after relapses had occurred. In the other four patients TCZ was continuously administered from the beginning at a dose of 8 mg/kg body weight at regular 4-weeks intervals. On some occasions, intervals between TCZ administrations were prolonged, e.g. due to holidays, missed appointments, or patients' wish. Only 2/8 patients received add-on therapy with monthly steroid pulses (temporary) or azathioprine, respectively, whereas the other 6 patients received TCZ as monotherapy (Figure 25).

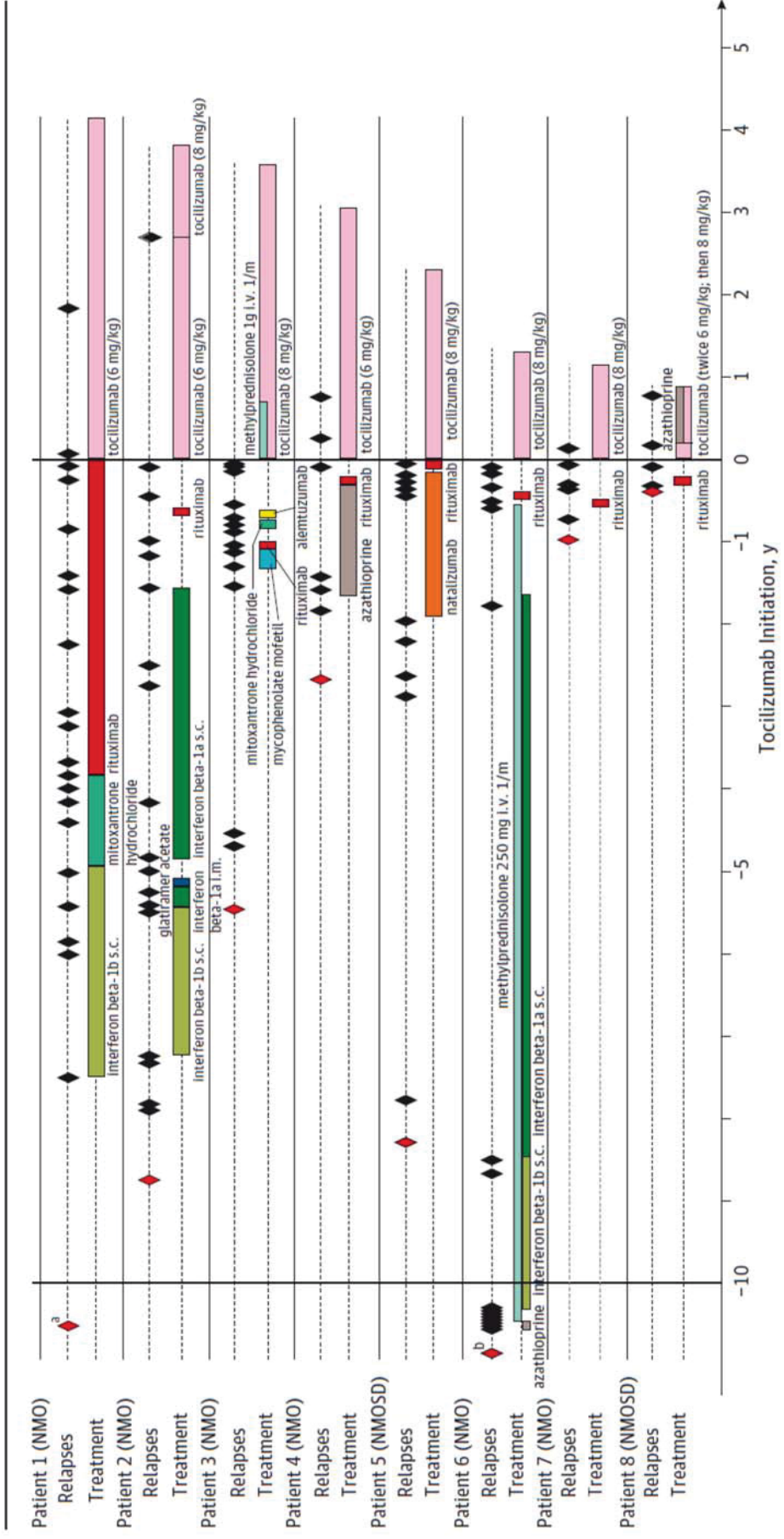


**Figure 25:** Disease course and immunomodulatory/immunosuppressant therapies of AQP4-Ab positive NMO/NMOSD patients. Clinical relapses (black diamonds, with first attacks in red diamonds) and treatments are shown. i.m.: intramuscular, i.v.: intravenous, s.c.: subcutaneous, 1/m: once per month. a: Twelve years before tocilizumab initiation. b: Twenty-four years before tocilizumab initiation (from [Ringelstein, Ayzenberg, Harmel, Lauenstein, Lensch, Stogbauer, Hellwig, Ellrichmann, Stettner, Chan, Hartung, Kieseier, Gold, Aktas, and Kleiter2015b]; see above publication No. 7).

The primary outcome measures were the annualized relapse rate (ARR), the EDSS, pain levels according to a numerical rating scale ranging from 0 (no pain) to 10 (intolerable pain) and AQP4-Ab titers tested by a cell-based assay prior to TCZ initiation and during the last three TCZ treatment months. Furthermore, 1.5 Tesla MRI scans with gadolinium administration of the cervico-thoracal spinal cord (sMRI) and the cranium (cMRI), performed at TCZ onset and at least once per year, as well as routine laboratory tests were analyzed.

The patients with a mean age at disease onset of  $29.4 \pm 9.9$  (mean  $\pm$  SD) years and of  $37.3 \pm 9.1$  years at first TCZ administration were followed-up for  $30.9 \pm 15.9$  months after switch to TCZ. All patients presented with high disease activity, represented by a median ARR of 2.0 (1.3-4.8; for the entire disease duration before TCZ) and 4.0 (3.0-5.0; for the last year before TCZ), respectively, and failed on previous medications, including rituximab. During TCZ treatment the median ARR significantly decreased from 4.0 (interquartile range 3.0-5.0) in the last year prior to TCZ to 0.365 (0-0.785) ( $p=0.0078$ ; Figure 26). Three patients remained relapse-free during TCZ treatment. In 5 patients a total of 8 relapses occurred, 4 within the first 2.5 months of therapy. Five attacks were associated with delayed TCZ administration (delay  $\geq 40$  days) and six bouts occurred with reduced TCZ dosage (6 mg/kg instead of 8 mg/kg).

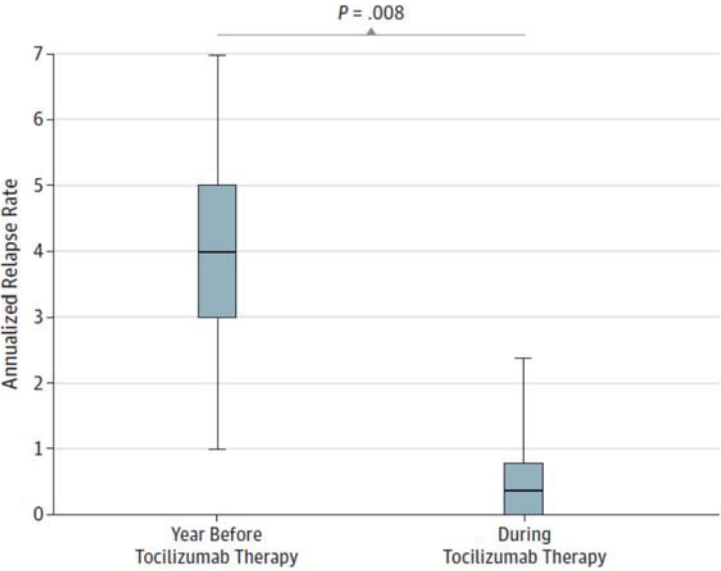


**Figure 26:** Annualized relapse rate (ARR) prior and during tocilizumab (TCZ) therapy. The median ARR significantly decreased from 4.0 (interquartile range, 3.0-5.0) in the year before TCZ therapy to 0.4 (interquartile range, 0.0-0.8) during TCZ therapy ( $P=0.008$ ) (from [Ringelstein et al. 2015b]; see above publication No. 7).

Between TCZ initiation and last follow-up during TCZ treatment the median EDSS dropped from 7.25 (5.375-8.375) to 5.5 (2.625-6.5) ( $p=0.0313$ ) (Figure 27). Six patients had a lower EDSS at last follow-up and no patient deteriorated. Active MRI lesions appeared in 6/8 patients at TCZ onset and in 1/8 at last MRI. AQP4-ab titers dropped significantly from a median of 1:1000 to 1:66 ( $p=0.0156$ ) and pain levels decreased significantly from median 6.5 (5.0-7.0) at onset of TCZ therapy to 2.5 (0.25-4.5) at last follow-up ( $p=0.0156$ ; Figure 27). Seven of eight patients had less pain, two of them were completely pain-free at last follow-up, with four patients still receiving continuous pain medication.

Adverse events during TCZ treatment included moderate cholesterol elevation in 6/8 patients, infections in 4/8, and deep venous thrombosis and neutropenia in one patient each. However, no severe infections or TCZ-related major adverse effects occurred.

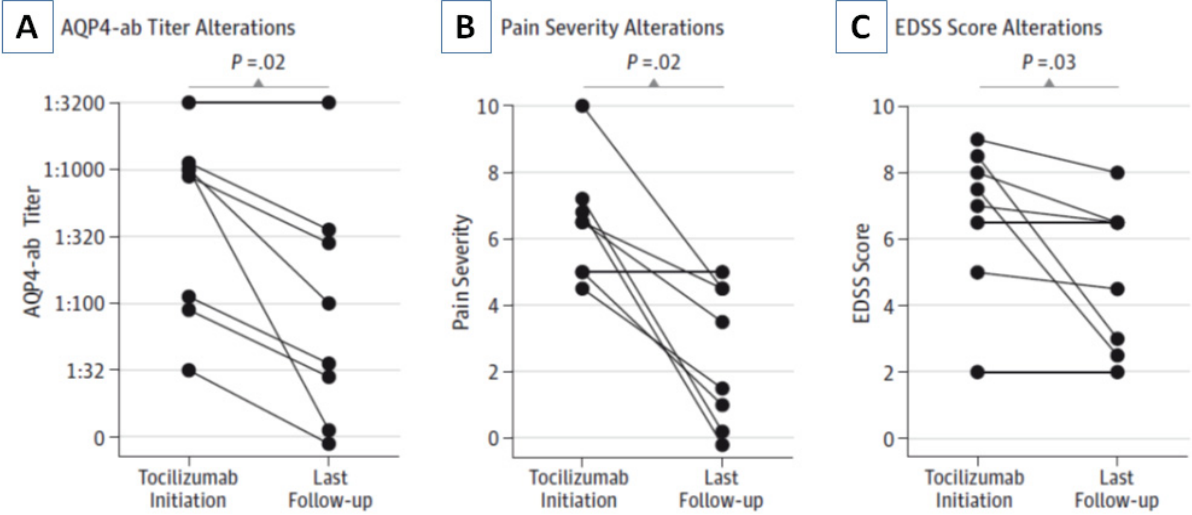


**Figure 27:** Features of disease activity prior and during tocilizumab (TCZ) therapy. Significant decrease of aquaporin-4 antibody (AQP4-ab) titers (A), pain levels assessed by a numeric rating scale (from 0-10; B), and the EDSS score (C) in NMOSD patients between start of TCZ therapy and last follow-up (modified from [Ringelstein et al. 2015b]; see above publication No. 7).

In summary, long-term TCZ mono-therapy in Caucasian patients with highly active NMO/NMOSD appears to be safe and effective in reducing the relapse rate in otherwise treatment resistant patients, particularly in rituximab non-responders. Similarly, further clinical (i.a. EDSS and pain levels) as well as paraclinical parameters

(i.a. MRI scans and AQP4-Ab titers) significantly improved during TCZ treatment. In this context it is important to mention, that the decrease of the EDSS in 6/8 patients and of the AQP4-Ab titers in 7/8 cases could have been influenced by the fact, that the initial values were ascertained shortly after an attack, when TCZ was started, and the final results during a remission phase. Moreover, one has to keep in mind that long-lasting biological effects of the preceding immunotherapies, such as rituximab, may have overlapped with the subsequent TCZ effects.

However, in summary, in the absence of a randomized controlled trial, our study suggests that TCZ is highly effective in otherwise treatment resistant NMOSD patients, when administered following a rather dense therapeutic regime with infusions every 28 days at a dosage of 8 mg/kg body weight. A reduced dosage of 6 mg/kg body weight and a prolonged TCZ administration interval of  $\geq 40$  days seem to increase the risk of relapses, preferentially during the first 2-3 months of treatment.

## **10. Summary, conclusion and outlook**

Neuro-axonal degeneration is the key feature in the pathogenesis of primarily neurodegenerative disorders but also occurs as a secondary phenomenon in inflammatory and vascular CNS diseases. As a result of CNS degeneration, being not reversible but possibly preventable in most of the diseases, the patient's disease burden and disability tend to increase, and the economic costs are tremendous. Thus, non-invasive, easy-applicable and cost-effective diagnostic tools such as OCT are highly appreciated to quantify and to follow-up axonal and neuronal cell loss for as early as possible diagnosis and in the light of therapeutic decisions. This is particularly true in "rare diseases" with their tendency to be underdiagnosed or even neglected.

This thesis highlights the diagnostic value of SD-OCT in primary neuroinflammatory (MS), neurodegenerative (ALS) and neurovascular (SuS) diseases in comparison to healthy controls or important differential diagnoses. Moreover, we evaluated the impact of diagnostic spinal cord biopsies and VEPs in NMOSD patients and analyzed the long-term efficacy and safety of Tocilizumab in these patients to answer the initially raised questions:

1. Our first OCT study in MS patients demonstrated a significant reduction of the RNFL and the TMV compared to HCs in patients both with and without previous ON [Brandt et al. 2011]. Our 2012 SD-OCT study confirmed these previous findings, but also carved out distinct OCT patterns in RRMS, SPMS and PPMS subtypes [Oberwahrenbrock et al. 2012; above publication No. 1]. In the same year we published one of the first studies that analyzed the deeper retinal layers in high-resolution SD-OCT scans [Albrecht et al. 2012c; above publication No. 2]. Besides a reduction of the RNFL and GCIPL complex in all MS subtypes, highlighting axonal *and* neuronal degeneration, we also found a thinning of the INL, exclusively in PPMS patients, suggesting a primary retinal pathology in contrast to a retrograde trans-synaptic degeneration after ON. Finally, we detected by SD-OCT a primary neuronal cell loss in eyes of patients with CIS, justifying treatment interventions already in this earliest stage of MS [Oberwahrenbrock et al. 2013; above publication No. 3].

As opposed to neuro-inflammatory MS, we investigated patients with ALS, a classical primary neurodegenerative motor neuron disease [Ringelstein et al. 2014b; above publication No. 4]. Here, SD-OCT for the first time revealed subtle reductions of the macular thickness and the RNFL as well as a marked thinning of the INL, highlighting the neuro-ophthalmologic involvement in ALS and giving further insights into the pathophysiology of the disease.

Finally, with SD-OCT we characterized the retinal pathology in patients with SuS, a rare micro-vascular disease of the retina, brain, and inner ear and an important differential diagnosis of MS [Ringelstein et al. 2015a; above publication No. 8]. Distinct OCT patterns of scattered, scar-like intraretinal damage in SuS eyes suggest a retinal, in contrast to a choroidal vascular pathomechanism and clearly differentiate SuS from MS patients. Depending on the disease stage, SD-OCT and fluorescein angiography provide important complementary diagnostic information to accelerate the correct diagnosis and prompt early treatment.

2. Diagnostic spinal cord biopsies in NMOSD patients resulted in serious postoperative complications and did not even lead to the correct diagnosis in the majority of cases. AQP4-Ab testing is mandatory in patients with inconclusive LESCL prior to spinal biopsy, which should be restricted to otherwise inconclusive

cases (Ringelstein et al. 2014d; above publication No. 6). Considering VEP latency prolongations and amplitude reductions, we were not able to define a distinct NMO pattern, as suggested by others, but found prolonged latencies in eyes without prior ON, indicating a subclinical affection [Ringelstein et al. 2014c; above publication No. 5].

3. Long-term IL-6 receptor blockade with tocilizumab, significantly reduces the ARR, EDSS, AQP4-Ab titers and pain levels without relevant adverse effects in highly active NMOSD patients, when administered following a strict therapeutic regimen [Ringelstein et al. 2015b; above publication No. 7].

Taken together, SD-OCT reliably detects neuro-axonal loss in primary neuroinflammatory, neurodegenerative and neurovascular diseases and facilitates the early diagnosis in several i.a. “orphan diseases”. As OCT is a non-invasive, safe, and highly precise diagnostic tool, we expect an increasing impact of OCT on the future differential diagnostic workup in various neurological disorders. In this context, we are currently preparing a first approach of diagnostic criteria for SuS, where SD-OCT should play an important role for the detection of retinal involvement of the disease.

Tocilizumab revealed an excellent efficacy/safety balance and can be considered a promising future therapy in highly disease active NMOSD patients, particularly in rituximab non-responders. Diagnostic spinal cord biopsies in NMOSD patients should be avoided or at least restricted to specific AQP4-Ab seronegative cases with no other diagnostic options. Longitudinal VEP studies in NMOSD are currently ongoing to further investigate subclinical disease processes and differential diagnostic issues.

## **11. German Summary (Zusammenfassung)**

Neuro-axonale Degeneration ist eines der Hauptmerkmale in der Pathogenese primär neurodegenerativer Erkrankungen, tritt aber auch als sekundäres Phänomen im Rahmen neuro-inflammatorischer und neuro-vaskulärer Erkrankungen des zentralen Nervensystems (ZNS) auf. Als Folge dieses neuro-axonalen Zelluntergangs im ZNS, der meist nicht reversibel, teilweise aber therapeutisch vermeidbar oder aufhaltbar ist, kommt es im allgemeinen zu einer Zunahme der Behinderung mit damit

einhergehender Einschränkung der Lebensqualität des Patienten und zu einem Anstieg der krankheitsbedingten Kosten. Daher sind nicht-invasive, anwenderfreundliche und kostengünstige Biomarker und Diagnostika, wie die optische Kohärenztomographie (OCT) erstrebenswert, die in der Lage ist axonalen und neuronalen Zelluntergang querschnittlich, aber auch longitudinal einfach und schnell zu quantifizieren, um so eine möglichst frühe Diagnose zu sichern und therapeutische Interventionen zu ermöglichen. Dies betrifft insbesondere die sogenannten „seltenen Erkrankungen“ (in der Europäischen Union definiert als Erkrankungen mit einer Prävalenz von  $< 5/10.000$  Einwohnern), die häufig fehl- oder unterdiagnostiziert sind und auch aufgrund ökonomischer Überlegungen meist therapeutisch vernachlässigt werden.

Der Hauptteil dieser Arbeit (d.h. die o.g. Publikationen 1-4 und 8) untersucht und beurteilt die Quantifizierbarkeit neuro-axonalen Zelluntergangs in jeweils einer primär neuroinflammatorischen Krankheit (Multiple Sklerose (MS)), einer neurodegenerativen Krankheit (Amyotrophe Lateralsklerose (ALS)) und einer seltenen neurovaskulären Krankheit (Susac Syndrome (SuS)) mittels OCT der Retina, einem evolutionsgeschichtlich vorgestülpten Teil des Gehirns. Die Spektral-Domänen OCT (SD-OCT) ist eine einfach anwendbare, nicht-invasive Untersuchungsmethode mit höchster anatomischer Auflösung im Mikrometerbereich zur Beurteilung primärer und sekundärer neuro-retinaler Erkrankungen. Die Sehbahn (insbesondere der Sehnerv und die Retina) stellt dabei eine ideale und leicht erfassbare, anatomische Struktur zum Nachweis von Neurodegeneration des Gehirns dar, da sowohl funktionelle, als auch strukturelle Messverfahren wie das Niedrig-Kontrastsehen, visuell evozierte Potentiale (VEP) und unterschiedliche OCT-Parameter u.a. mit dem Grad der Hirnatrophie im MRT, aber auch mit dem Grad der Behinderung und der Lebensqualität z.B. bei MS Patienten eng korrelieren [Balcer et al. 2015].

Die o.g. Publikationen 5-7 beschäftigen sich darüber hinaus mit (differential-) diagnostischen Aspekten (Rückenmarksbiopsie und VEP), aber auch mit einer vielversprechenden neuen Therapieoption (Tocilizumab) bei Patienten mit Neuromyelitis optica Spektrumerkrankungen (NMOSD).

Bemerkenswerterweise handelt es sich im Gegensatz zur häufigen MS [Compston and Coles 2008] sowohl bei der hier untersuchten ALS [Kiernan et al. 2011], als auch dem

SuS [Dörr et al. 2013a] und den NMOSD [Wingerchuk and Weinshenker 2014], um „seltene Erkrankungen“ mit Prävalenzen von unter 1/10.000 Einwohnern.

Vor diesem Hintergrund versuchen die in dieser kumulativen Habilitationsschrift dargestellten wissenschaftlichen Untersuchungen der letzten Jahre folgende drei Fragen zu beantworten:

1. Kann die SD-OCT zuverlässig neuro-axonale Degeneration in primär neuroinflammatorischen (MS), neurodegenerativen (ALS) und neurovaskulären (SuS) Erkrankungen erfassen und quantifizieren, und kann sie differentialdiagnostische Hilfe z.B. bei der Differenzierung des SuS gegenüber der MS leisten?
2. Welchen (differential-) diagnostischen Nutzen haben die Rückenmarksbiopsie und die VEP bei Patienten mit NMOSD?
3. Stellt die Langzeittherapie durch Interleukin-6 Rezeptorblockade mittels Tocilizumab eine effektive und gleichzeitig sichere Behandlungsalternative für hochaktive NMOSD Patienten dar?

Um diese Fragen zu beantworten, untersuchten wir mittels neuester SD-OCT Technologie die bis dato größten Patientenkollektive mit unterschiedlichen MS Subtypen, definitiver ALS und SuS und verglichen die Untersuchungsergebnisse mit denen gesunder Kontrollen, aber auch untereinander. Darüber hinaus beurteilten wir erstmals die differentialdiagnostische Bedeutung von Rückenmarksbiopsien und VEP sowie die Wirksamkeit und Sicherheit von Tocilizumab in den bis dahin größten in der Literatur beschriebenen Kohorten kaukasischer NMOSD Patienten.

1. Unsere erste SD-OCT Studie an MS Patienten zeigte eine signifikante Reduktion der retinalen Nervenfaserschicht (RNFL) und des gesamtmakulären Volumens (TMV) bei Patienten mit, aber auch ohne vorherige Optikusneuritis (ON) im Vergleich zu gesunden Kontrollen [Brandt et al. 2011]. Unsere 2012 veröffentlichte SD-OCT Studie bestätigte diese Ergebnisse und konnte darüber hinaus unterschiedliche OCT-Muster für die verschiedenen MS-Verlaufstypen (RRMS: schubförmige MS, SPMS: sekundär-progrediente MS, PPMS: primär progrediente

MS) charakterisieren [Oberwahrenbrock et al. 2012; o.g. Publikation Nr. 1]. Im gleichen Jahr publizierten wir eine der weltweit ersten Studien, die mittels SD-OCT auch die tieferen retinalen Schichten beurteilte [Albrecht et al. 2012c; o.g. Publikation Nr. 2]. Neben einer Schichtdickenreduktion der RNFL und der Ganglienzell-/inneren plexiformen Schicht (GCIPL) in allen MS-Subtypen als Hinweis auf eine axonale (RNFL) und neuronale (GCIPL) Degeneration, konnten wir auch eine Ausdünnung der inneren nukleären Schicht (INL), ausschließlich bei PPMS Patienten ohne frühere ON nachweisen, die den Verdacht auf eine primär retinale Pathologie, im Gegensatz zu einer retrograden trans-synaptischen Degeneration, nahelegen. Abschließend gelang uns mittels SD-OCT erstmals der Nachweis eines primär neuro-retinalen Zelluntergangs bereits im Stadium des klinisch isolierten Syndroms (CIS), dem potentiell ersten, klinisch erkennbaren Stadium einer MS. Hieraus lässt sich u.a. eine Rechtfertigung für einen sehr frühen Behandlungsbeginn einer MS ableiten [Oberwahrenbrock et al. 2013; o.g. Publikation Nr. 3].

Im Gegensatz zur primär neuroinflammatorischen MS, untersuchten wir auch Patienten mit ALS, einer klassischen neurodegenerativen Erkrankung vor allem der Motoneurone [Ringelstein et al. 2014b; o.g. Publikation Nr. 4]. Unsere SD-OCT Untersuchungen konnten erstmals eine leichte Reduktion der makulären Dicke und der RNFL sowie eine deutliche Ausdünnung der INL aufzeigen. Diese Ergebnisse bestätigen eine u.a. aus Autopsie- und MRT-Studien anderer Arbeitsgruppen vermutete, neuroophthalmologische Beteiligung bei der ALS und erweitern dadurch das pathophysiologische Verständnis dieser Erkrankung.

In einem dritten Schritt konnten wir mit Hilfe der SD-OCT retinale Pathologien bei Patienten mit SuS, einer seltenen mikrovaskulären Erkrankung des Gehirns, der Retina und des Innenohrs, und gleichzeitig einer wichtigen Differentialdiagnose der MS, nachweisen [Ringelstein et al. 2015a; o.g. Publikation Nr. 8]. Charakteristische OCT-Veränderungen der SuS-Augen mit ausgeprägten fleckförmig verteilten, narbenartigen Schädigungen der inneren Netzhautschichten unterstreichen den retinalen, im Gegensatz zu einem choroidalen vaskulären Pathomechanismus, und sie unterscheiden sich grundlegend von OCT-Veränderungen der MS Patienten. Abhängig vom Krankheitsstadium stellen somit die SD-OCT (in der langen Remissionsphase) und die Fluoreszenzangiographie (in der kurzen Akutphase)

gleichwertige diagnostische Untersuchungsmethoden zur Diagnosesicherung des Susac Syndroms dar.

2. Diagnostische Rückenmarksbiopsien von Patienten mit unklarer langstreckiger Rückenmarkspathologie, die schlussendlich als NMOSD diagnostiziert wurden, gingen häufig mit schweren postoperativen Komplikationen einher und konnten in den meisten Fällen trotz ihrer Invasivität doch nicht zur Diagnosefindung beitragen (Ringelstein et al. 2014d; o.g. Publikation Nr. 6). Eine serologische Aquaporin-4 Antikörper (AQP4-Ak) Testung ist daher bei Patienten mit langstreckigen Myelonauffälligkeiten *vor* einer spinalen Biopsie, die nur in sehr seltenen, ausgewählten Fällen durchgeführt werden sollte, zwingend erforderlich.

Unter Berücksichtigung von VEP-Latenzen und -Amplituden konnten wir das von einer anderen Arbeitsgruppe vorgeschlagene eigene „NMO-Muster“ in unserem deutlich größeren und besser definierten NMOSD-Kollektiv nicht bestätigen, fanden aber u.a. verzögerte P100-Latenzen in Augen ohne vorbeschriebene ON, als möglichen Hinweis auf eine subklinische Sehnervenbeteiligung [Ringelstein et al. 2014c; o.g. Publikation Nr. 5].

3. Eine langfristige Interleukin-6 Rezeptor Blockade mittels Tocilizumab reduzierte bei Patienten mit hochaktiver NMOSD die jährliche Schubrate, den Grad der Behinderung, AQP4-Ak Titer sowie Schmerzen signifikant, ohne dass es gleichzeitig zu relevanten Nebenwirkungen kam. Tocilizumab sollte monatlich in einer Dosierung von 8 mg/kg Körpergewicht verabreicht werden [Ringelstein et al. 2015b; o.g. Publikation Nr. 7].

Zusammenfassend konnten wir zeigen, dass die Spektral-Domänen OCT zuverlässig retinale neuro-axonale Degeneration infolge neuroinflammatorischer, neurodegenerativer und neurovaskulärer Erkrankungen nachweisen und quantifizieren kann und so zur korrekten, möglicherweise früheren Diagnosefindung selbst bei “orphan diseases” beitragen kann. Da die OCT-Untersuchung höchst präzise, nicht-invasiv und gut reproduzierbar ist, rechnen wir in den kommenden Jahren mit einem zunehmenden Stellenwert der OCT in der differentialdiagnostischen Abklärung neurologischer Erkrankungen. In diesem Zusammenhang bereiten wir

derzeit erste Diagnosekriterien für das SuS vor, bei denen die SD-OCT eine wichtige Rolle zum Nachweis der krankheitstypischen retinalen Beteiligung spielen soll.

Tocilizumab zeigte in unserer Studie ein exzellentes Wirkungs-/Nebenwirkungsprofil und kann als äußerst vielversprechende und zukunftssträchtige Therapie der NMOSD bei hoher Krankheitsaktivität angesehen werden. Diagnostische Rückenmarksbiopsien von Patienten mit langstreckiger unklarer Myelopathie sollten unter dem differentialdiagnostischen Verdacht auf eine NMOSD in jedem Fall erst nach einer AQP4-Ak Testung erwogen werden und bei negativem Serumergebnis sowie Versagen weiterer Diagnostika auf dezidierte Einzelfälle beschränkt bleiben. Eine VEP-Longitudinalstudie bei NMOSD Patienten wird derzeit durchgeführt und kann uns eventuell weitere Aufschlüsse über subklinische Krankheitsaktivität und den differentialdiagnostischen Nutzen dieses Ansatzes geben.

## **12. Acknowledgement**

I would like to thank Prof. Hans-Peter Hartung, Chairman of the Dpt. of Neurology, Heinrich-Heine-University (HHU) in Düsseldorf, for his continuous interest and academic support. I would like to especially thank Prof. Orhan Aktas, who, as scientific mentor and head of our academic group, always supported me, introduced me to Neuromyelitis optica and taught me excel independently in the scientific community.

My special thank goes to our technician, Eva Cohn, and my PhD students Nazmiye Keser and Björn Bühn for their diligent and unstintingly support, without which the enormous amount of work would not have been possible. I would also like to warmly thank my esteemed colleagues and contributors of our working group PD Dr. Philipp Albrecht, Jens Harmel, Ann-Kristin Müller and Dr. Jens Ingwersen for many fruitful discussions and their continuous support in solving various problems.

Furthermore, I would like to thank our cooperation partners Dr. David Finis and Prof. Rainer Guthoff (Dpt. of Ophthalmology, HHU), Dr. Christian Mathys (Dpt. of Diagnostic and Interventional Radiology, HHU), Dr. Stefano Ferrea, PD Dr. Martin Südmeyer and Prof. Alfons Schnitzler (Institute of Clinical Neuroscience and Medical Psychology, HHU), Prof. Axel Methner (Dpt. of Neurology, Johannes-Gutenberg University, Mainz), Prof. Sven Schippling (Dpt. of Neurology, University Hospital, Zürich), Dr. Ilka Kleffner

and Prof. Thomas Duning (Dpt. of Neurology, University Hospital, Münster), Timm Oberwahrenbrock, Dr. Alexander Brandt, Dr. Jan Dörr, PD Dr. Klemens Ruprecht and Prof. Friedemann Paul (Dpt. of Neurology and NeuroCure Clinical Research Center, Charité, Berlin), PD Dr. Markus Krämer (Alfried Krupp Hospital, Essen), Dr. Ilya Ayzenberg, PD Dr. Kerstin Hellwig and Prof. Ingo Kleiter (Dpt. of Neurology, St Josef Hospital, Ruhr University, Bochum), Dr. Sven Jarius and Prof. Brigitte Wildemann (Dpt. of Neurology and Division of Molecular Neuroimmunology, University Hospital, Heidelberg) as well as all the other members of the Neuromyelitis optica Studiengruppe (NEMOS; [www.nemos-net.de](http://www.nemos-net.de)) and the European Susac Consortium (EUSAC; [www.eusac.net](http://www.eusac.net)) for productive collaborations.

Last, but certainly not least, I would like to warmly thank my parents Prof. Dr. Dr. E. Bernd Ringelstein and Hannelore Ringelstein-Wirz for their perpetual encouragement and insight, as well as my wife Nina and my children Leona Sophie, Julian Louis and Linus Johann for their endless patience and support.

### 13. Reference List

Abraham A, Drory VE. Fatigue in motor neuron diseases. *Neuromuscul Disord* 2012; 22 Suppl 3: S198-S202.

Albrecht P, Blasberg C, Lukas S *et al.* Retinal pathology in idiopathic moyamoya angiopathy detected by optical coherence tomography. *Neurology* 2015; 85: 521-527.

Albrecht P, Muller AK, Ringelstein M *et al.* Retinal neurodegeneration in Wilson's disease revealed by spectral domain optical coherence tomography. *PLoS One* 2012a; 7: e49825.

Albrecht P, Muller AK, Sudmeyer M *et al.* Optical coherence tomography in parkinsonian syndromes. *PLoS One* 2012b; 7: e34891.

Albrecht P, Ringelstein M, Muller AK *et al.* Degeneration of retinal layers in multiple sclerosis subtypes quantified by optical coherence tomography. *Mult Scler* 2012c; 18: 1422-1429.

Arnold AC. Evolving management of optic neuritis and multiple sclerosis. *Am J Ophthalmol* 2005; 139: 1101-1108.

Balcer L, Miller D, Reingold S *et al.* Vision and vision-related outcome measures in multiple sclerosis. *Brain* 2015; 138: 11-27.

Bede P, Bokde A, Elamin M *et al.* Grey matter correlates of clinical variables in amyotrophic lateral sclerosis (ALS): a neuroimaging study of ALS motor phenotype heterogeneity and cortical focality. *J Neurol Neurosurg Psychiatry* 2013; 84: 766-73.

Brandt AU, Oberwahrenbrock T, Ringelstein M *et al.* Primary retinal pathology in multiple sclerosis as detected by optical coherence tomography. *Brain* 2011; 134: e193.

Brandt AU, Zimmermann H, Kaufhold F *et al.* Patterns of retinal damage facilitate differential diagnosis between Susac syndrome and MS. *PLoS One* 2012a; 7: e38741.

Brettschneider J, Del TK, Toledo JB *et al.* Stages of pTDP-43 pathology in amyotrophic lateral sclerosis. *Ann Neurol* 2013; 74: 20-38.

Brettschneider J, Petzold A, Sussmuth SD, Ludolph AC, Tumani H. Axonal damage markers in cerebrospinal fluid are increased in ALS. *Neurology* 2006; 66: 852-856.

Burkholder BM, Osborne B, Loguidice MJ *et al.* Macular volume determined by optical coherence tomography as a measure of neuronal loss in multiple sclerosis. *Arch Neurol* 2009; 66: 1366-1372.

Byrne S, Elamin M, Bede P *et al.* Cognitive and clinical characteristics of patients with amyotrophic lateral sclerosis carrying a C9orf72 repeat expansion: a population-based cohort study. *Lancet Neurol* 2012; 11: 232-240.

Cauberg EC, de Bruin DM, Faber DJ, van Leeuwen TG, de la Rosette JJ, de Reijke TM. A new generation of optical diagnostics for bladder cancer: technology, diagnostic accuracy, and future applications. *Eur Urol* 2009; 56: 287-296.

Chihara N, Aranami T, Sato W *et al.* Interleukin 6 signaling promotes anti-aquaporin 4 autoantibody production from plasmablasts in neuromyelitis optica. *Proc Natl Acad Sci U S A* 2011; 108: 3701-3706.

Compston A, Coles A. Multiple sclerosis. *Lancet* 2008; 372: 1502-1517.

Costa J, Swash M, de CM. Awaji criteria for the diagnosis of amyotrophic lateral sclerosis: a systematic review. *Arch Neurol* 2012; 69: 1410-1416.

Costello F, Hodge W, Pan YI, Eggenberger E, Coupland S, Kardon RH. Tracking retinal nerve fiber layer loss after optic neuritis: a prospective study using optical coherence tomography. *Mult Scler* 2008; 14: 893-905.

De Stefano N, Giorgio A, Battaglini M *et al.* Assessing brain atrophy rates in a large population of untreated multiple sclerosis subtypes. *Neurology* 2010; 74: 1868-1876.

Dörr J, Krautwald S, Wildemann B *et al.* Characteristics of Susac syndrome: a review of all reported cases. *Nat Rev Neurol* 2013a; 9: 307-316.

Dörr J, Ringelstein M, Duning T, Kleffner I. Update on Susac syndrome: new insights in brain and retinal imaging and treatment options. *J Alzheimers Dis* 2014; 42 Suppl 3: S99-108.

Drexler W, Morgner U, Ghanta RK, Kartner FX, Schuman JS, Fujimoto JG. Ultrahigh-resolution ophthalmic optical coherence tomography. *Nat Med* 2001; 7: 502-507.

Egan RA, Hills WL, Susac JO. Gass plaques and fluorescein leakage in Susac Syndrome. *J Neurol Sci* 2010; 299: 97-100.

Elsone L, Kitley J, Luppe S *et al.* Long-term efficacy, tolerability and retention rate of azathioprine in 103 aquaporin-4 antibody-positive neuromyelitis optica spectrum disorder

patients: a multicentre retrospective observational study from the UK. *Mult Scler* 2014; 20: 1533-40.

Fairless R, Williams SK, Hoffmann DB *et al.* Preclinical retinal neurodegeneration in a model of multiple sclerosis: *The Journal of Neuroscience* 2012; 32(16):5585-5597. *Ann Neurosci* 2012; 19: 121-122.

Filippi M, Bozzali M, Rovaris M *et al.* Evidence for widespread axonal damage at the earliest clinical stage of multiple sclerosis. *Brain* 2003; 126: 433-437.

Fischer MD, Synofzik M, Heidlaufer R *et al.* Retinal nerve fiber layer loss in multiple system atrophy. *Mov Disord* 2011; 26: 914-916.

Graves J, Balcer LJ. Eye disorders in patients with multiple sclerosis: natural history and management. *Clin Ophthalmol* 2010; 4: 1409-1422.

Green AJ, McQuaid S, Hauser SL, Allen IV, Lyness R. Ocular pathology in multiple sclerosis: retinal atrophy and inflammation irrespective of disease duration. *Brain* 2010; 133: 1591-1601.

Habeck C, Foster NL, Pernecky R *et al.* Multivariate and univariate neuroimaging biomarkers of Alzheimer's disease. *Neuroimage* 2008; 40: 1503-1515.

Halliday AM, McDonald WI, Mushin J. Visual evoked response in diagnosis of multiple sclerosis. *Br Med J* 1973; 4: 661-664.

Hampel H, Goernitz A, Buerger K. Advances in the development of biomarkers for Alzheimer's disease: from CSF total tau and Aβ(1-42) proteins to phosphorylated tau protein. *Brain Res Bull* 2003; 61: 243-253.

Harmel J, Ringelstein M, Ingwersen J *et al.* Interferon-beta-related tumefactive brain lesion in a Caucasian patient with neuromyelitis optica and clinical stabilization with tocilizumab. *BMC Neurol* 2014; 14: 247.

Hashizume M, Tan SL, Takano J *et al.* Tocilizumab, A Humanized Anti-IL-6R Antibody, as an Emerging Therapeutic Option for Rheumatoid Arthritis: Molecular and Cellular Mechanistic Insights. *Int Rev Immunol* 2015; 34: 265-79.

Hauser SL, Chan JR, Oksenberg JR. Multiple sclerosis: Prospects and promise. *Ann Neurol* 2013; 74: 317-327.

Hein T, Hopfenmuller W. [Projection of the number of multiple sclerosis patients in Germany]. *Nervenarzt* 2000; 71: 288-294.

Henderson AP, Trip SA, Schlottmann PG *et al.* An investigation of the retinal nerve fibre layer in progressive multiple sclerosis using optical coherence tomography. *Brain* 2008; 131: 277-287.

Hong Z, Shi M, Chung KA *et al.* DJ-1 and alpha-synuclein in human cerebrospinal fluid as biomarkers of Parkinson's disease. *Brain* 2010; 133: 713-726.

Huang D, Swanson EA, Lin CP *et al.* Optical coherence tomography. *Science* 1991; 254: 1178-1181.

Huh SY, Kim SH, Hyun JW *et al.* Mycophenolate Mofetil in the Treatment of Neuromyelitis Optica Spectrum Disorder. *JAMA Neurol* 2014; 71: 1372-8.

Izatt JA, Hee MR, Swanson EA *et al.* Micrometer-scale resolution imaging of the anterior eye in vivo with optical coherence tomography. *Arch Ophthalmol* 1994; 112: 1584-1589.

Jarius S, Franciotta D, Paul F *et al.* Testing for antibodies to human aquaporin-4 by ELISA: sensitivity, specificity, and direct comparison with immunohistochemistry. *J Neurol Sci* 2012a; 320: 32-37.

Jarius S, Kleffner I, Dorr JM *et al.* Clinical, paraclinical and serological findings in Susac syndrome: an international multicenter study. *J Neuroinflammation* 2014a; 11: 46.

Jarius S, Paul F, Fechner K *et al.* Aquaporin-4 antibody testing: direct comparison of M1-AQP4-DNA-transfected cells with leaky scanning versus M23-AQP4-DNA-transfected cells as antigenic substrate. *J Neuroinflammation* 2014b; 11: 129.

Jarius S, Paul F, Franciotta D *et al.* Cerebrospinal fluid findings in aquaporin-4 antibody positive neuromyelitis optica: results from 211 lumbar punctures. *J Neurol Sci* 2011; 306: 82-90.

Jarius S, Probst C, Borowski K *et al.* Standardized method for the detection of antibodies to aquaporin-4 based on a highly sensitive immunofluorescence assay employing recombinant target antigen. *J Neurol Sci* 2010; 291: 52-56.

Jarius S, Ruprecht K, Wildemann B *et al.* Contrasting disease patterns in seropositive and seronegative neuromyelitis optica: A multicentre study of 175 patients. *J Neuroinflammation* 2012b; 9: 14.

Kallenbach K, Sander B, Tsakiri A *et al.* Neither retinal nor brain atrophy can be shown in patients with isolated unilateral optic neuritis at the time of presentation. *Mult Scler* 2011; 17: 89-95.

Keltner JL, Johnson CA, Cello KE, Dontchev M, Gal RL, Beck RW. Visual field profile of optic neuritis: a final follow-up report from the optic neuritis treatment trial from baseline through 15 years. *Arch Ophthalmol* 2010; 128: 330-337.

Kiernan MC, Vucic S, Cheah BC *et al.* Amyotrophic lateral sclerosis. *Lancet* 2011; 377: 942-955.

Kim SH, Huh SY, Lee SJ, Joung A, Kim HJ. A 5-year follow-up of rituximab treatment in patients with neuromyelitis optica spectrum disorder. *JAMA Neurol* 2013; 70: 1110-1117.

Kitley J, Elson L, George J *et al.* Methotrexate is an alternative to azathioprine in neuromyelitis optica spectrum disorders with aquaporin-4 antibodies. *J Neurol Neurosurg Psychiatry* 2013; 84: 918-921.

Kitley JL, Leite MI, George JS, Palace JA. The differential diagnosis of longitudinally extensive transverse myelitis. *Mult Scler* 2012; 18: 271-285.

Kitley JL, Leite MI, Matthews LA, Palace J. Use of mitoxantrone in neuromyelitis optica. *Arch Neurol* 2011; 68: 1086-1087.

Kleffner I, Deppe M, Mohammadi S *et al.* Diffusion tensor imaging demonstrates fiber impairment in Susac syndrome. *Neurology* 2008; 70: 1867-1869.

Kleiter I, Gahlen A, Borisow N *et al.* Neuromyelitis optica: Evaluation of 871 attacks and 1153 treatment courses. *Ann Neurol* 2015.

Kleiter I, Hellwig K, Berthele A *et al.* Failure of natalizumab to prevent relapses in neuromyelitis optica. *Arch Neurol* 2012; 69: 239-245.

Kolb H. *Simple Anatomy of the Retina*. 1995.

Kurtzke JF. Rating neurologic impairment in multiple sclerosis: an expanded disability status scale (EDSS). *Neurology* 1983; 33: 1444-1452.

Lennon VA, Kryzer TJ, Pittock SJ, Verkman AS, Hinson SR. IgG marker of optic-spinal multiple sclerosis binds to the aquaporin-4 water channel. *J Exp Med* 2005; 202: 473-477.

Lennon VA, Wingerchuk DM, Kryzer TJ *et al.* A serum autoantibody marker of neuromyelitis optica: distinction from multiple sclerosis. *Lancet* 2004; 364: 2106-2112.

Lucchinetti CF, Mandler RN, McGavern D *et al.* A role for humoral mechanisms in the pathogenesis of Devic's neuromyelitis optica. *Brain* 2002; 125: 1450-1461.

Lucchinetti CF, Popescu BF, Bunyan RF *et al.* Inflammatory cortical demyelination in early multiple sclerosis. *N Engl J Med* 2011; 365: 2188-2197.

Matthews WB, Small DG, Small M, Pountney E. Pattern reversal evoked visual potential in the diagnosis of multiple sclerosis. *J Neurol Neurosurg Psychiatry* 1977; 40: 1009-1014.

McEvoy LK, Fennema-Notestine C, Roddey JC *et al.* Alzheimer disease: quantitative structural neuroimaging for detection and prediction of clinical and structural changes in mild cognitive impairment. *Radiology* 2009; 251: 195-205.

Min JH, Kim BJ, Lee KH. Development of extensive brain lesions following fingolimod (FTY720) treatment in a patient with neuromyelitis optica spectrum disorder. *Mult Scler* 2012; 18: 113-115.

Misu T, Fujihara K, Kakita A *et al.* Loss of aquaporin 4 in lesions of neuromyelitis optica: distinction from multiple sclerosis. *Brain* 2007; 130: 1224-1234.

Moss HE, McCluskey L, Elman L *et al.* Cross-sectional evaluation of clinical neuro-ophthalmic abnormalities in an amyotrophic lateral sclerosis population. *J Neurol Sci* 2012; 314: 97-101.

Munte TF, Troger MC, Nusser I *et al.* Alteration of early components of the visual evoked potential in amyotrophic lateral sclerosis. *J Neurol* 1998; 245: 206-210.

Neto SP, Alvarenga RM, Vasconcelos CC, Alvarenga MP, Pinto LC, Pinto VL. Evaluation of pattern-reversal visual evoked potential in patients with neuromyelitis optica. *Mult Scler* 2013; 19: 173-178.

Oberwahrenbrock T, Ringelstein M, Jentschke S *et al.* Retinal ganglion cell and inner plexiform layer thinning in clinically isolated syndrome. *Mult Scler* 2013; 19: 1887-1895.

Oberwahrenbrock T, Schippling S, Ringelstein M *et al.* Retinal damage in multiple sclerosis disease subtypes measured by high-resolution optical coherence tomography. *Mult Scler Int* 2012; 2012: 530305.

Olney NT, Goodkind MS, Lomen-Hoerth C *et al.* Behaviour, physiology and experience of pathological laughing and crying in amyotrophic lateral sclerosis. *Brain* 2011; 134: 3458-3469.

Outteryck O, Zephir H, Defoort S *et al.* Optical coherence tomography in clinically isolated syndrome: no evidence of subclinical retinal axonal loss. *Arch Neurol* 2009; 66: 1373-1377.

Parisi L, Rocca MA, Mattioli F *et al.* Patterns of regional gray matter and white matter atrophy in cortical multiple sclerosis. *J Neurol* 2014; 261: 1715-1725.

Parisi V, Manni G, Spadaro M *et al.* Correlation between morphological and functional retinal impairment in multiple sclerosis patients. *Invest Ophthalmol Vis Sci* 1999; 40: 2520-2527.

Parisi V, Restuccia R, Fattapposta F, Mina C, Bucci MG, Pierelli F. Morphological and functional retinal impairment in Alzheimer's disease patients. *Clin Neurophysiol* 2001; 112: 1860-1867.

Petzold A, de Boer JF, Schippling S *et al.* Optical coherence tomography in multiple sclerosis: a systematic review and meta-analysis. *Lancet Neurol* 2010; 9: 921-932.

Price S, Paviour D, Scahill R *et al.* Voxel-based morphometry detects patterns of atrophy that help differentiate progressive supranuclear palsy and Parkinson's disease. *Neuroimage* 2004; 23: 663-669.

Puliafito CA, Hee MR, Lin CP *et al.* Imaging of macular diseases with optical coherence tomography. *Ophthalmology* 1995; 102: 217-229.

Ramli N, Nair SR, Ramli NM, Lim SY. Differentiating multiple-system atrophy from Parkinson's disease. *Clin Radiol* 2015; 70: 555-564.

Ringelstein M, Aktas O, Harmel J *et al.* [Contribution of spinal cord biopsy to the differential diagnosis of longitudinal extensive transverse myelitis]. *Nervenarzt* 2014a; 85: 1298-1303.

Ringelstein M, Albrecht P, Kleffner I *et al.* Retinal pathology in Susac syndrome detected by spectral-domain optical coherence tomography. *Neurology* 2015a; 85: 610-618.

Ringelstein M, Albrecht P, Sudmeyer M *et al.* Subtle retinal pathology in amyotrophic lateral sclerosis. *Ann Clin Transl Neurol* 2014b; 1: 290-297.

Ringelstein M, Ayzenberg I, Harmel J *et al.* Long-term Therapy With Interleukin 6 Receptor Blockade in Highly Active Neuromyelitis Optica Spectrum Disorder. *JAMA Neurol* 2015b; 72: 756-763.

Ringelstein M, Harmel J, Distelmaier F *et al.* Neuromyelitis optica and pregnancy during therapeutic B cell depletion: infant exposure to anti-AQP4 antibody and prevention of rebound relapses with low-dose rituximab postpartum. *Mult Scler* 2013a; 19: 1544-1547.

Ringelstein M, Kleiter I, Ayzenberg I *et al.* Visual evoked potentials in neuromyelitis optica and its spectrum disorders. *Mult Scler* 2014c; 20: 617-20.

Ringelstein M, Lanzman R, Aktas O. Neuromyelitis optica - Diagnostik und Therapie. 2010; 2: 41-9.

Ringelstein M, Metz I, Ruprecht K *et al.* Contribution of spinal cord biopsy to diagnosis of aquaporin-4 antibody positive neuromyelitis optica spectrum disorder. *Mult Scler* 2014d; 20: 882-88.

Roth NM, Saidha S, Zimmermann H *et al.* Optical coherence tomography does not support optic nerve involvement in amyotrophic lateral sclerosis. *Eur J Neurol* 2013; 20: 1170-6.

Rufa A, Pretegianni E, Frezzotti P *et al.* Retinal nerve fiber layer thinning in CADASIL: an optical coherence tomography and MRI study. *Cerebrovasc Dis* 2011; 31: 77-82.

Saidha S, Syc SB, Ibrahim MA *et al.* Primary retinal pathology in multiple sclerosis as detected by optical coherence tomography. *Brain* 2011; 134: 518-533.

Schuman JS, Hee MR, Puliafito CA *et al.* Quantification of nerve fiber layer thickness in normal and glaucomatous eyes using optical coherence tomography. *Arch Ophthalmol* 1995; 113: 586-596.

Sharma R, Hicks S, Berna CM, Kennard C, Talbot K, Turner MR. Oculomotor dysfunction in amyotrophic lateral sclerosis: a comprehensive review. *Arch Neurol* 2011; 68: 857-861.

Shimizu J, Hatanaka Y, Hasegawa M *et al.* IFNbeta-1b may severely exacerbate Japanese optic-spinal MS in neuromyelitis optica spectrum. *Neurology* 2010; 75: 1423-1427.

Sotirchos ES, Seigo MA, Calabresi PA, Saidha S. Comparison of point estimates and average thicknesses of retinal layers measured using manual optical coherence tomography segmentation for quantification of retinal neurodegeneration in multiple sclerosis. *Curr Eye Res* 2013; 38: 224-228.

Stricker S, Oberwahrenbrock T, Zimmermann H *et al.* Temporal retinal nerve fiber loss in patients with spinocerebellar ataxia type 1. *PLoS One* 2011; 6: e23024.

Susac JO, Hardman JM, Selhorst JB. Microangiopathy of the brain and retina. *Neurology* 1979; 29: 313-316.

Susac JO, Murtagh FR, Egan RA *et al.* MRI findings in Susac's syndrome. *Neurology* 2003; 61: 1783-1787.

Swanson EA, Izatt JA, Hee MR *et al.* In vivo retinal imaging by optical coherence tomography. *Opt Lett* 1993; 18: 1864-1866.

Syc SB, Saidha S, Newsome SD *et al.* Optical coherence tomography segmentation reveals ganglion cell layer pathology after optic neuritis. *Brain* 2012; 135: 521-533.

Talman LS, Bisker ER, Sackel DJ *et al.* Longitudinal study of vision and retinal nerve fiber layer thickness in multiple sclerosis. *Ann Neurol* 2010; 67: 749-760.

Trapp BD, Nave KA. Multiple sclerosis: an immune or neurodegenerative disorder? *Annu Rev Neurosci* 2008; 31: 247-269.

Trebst C, Berthele A, Jarius S *et al.* [Diagnosis and treatment of neuromyelitis optica. Consensus recommendations of the Neuromyelitis Optica Study Group]. *Nervenarzt* 2011a; 82: 768-777.

Trebst C, Jarius S, Berthele A *et al.* Update on the diagnosis and treatment of neuromyelitis optica: Recommendations of the Neuromyelitis Optica Study Group (NEMOS). *J Neurol* 2014; 261: 1-16.

Trebst C, Raab P, Voss EV *et al.* Longitudinal extensive transverse myelitis--it's not all neuromyelitis optica. *Nat Rev Neurol* 2011b; 7: 688-698.

Trip SA, Schlottmann PG, Jones SJ *et al.* Retinal nerve fiber layer axonal loss and visual dysfunction in optic neuritis. *Ann Neurol* 2005; 58: 383-391.

Turkyilmaz K, Oner V, Turkyilmaz AK, Kirbas A, Kirbas S, Sekeryapan B. Evaluation of peripapillary retinal nerve fiber layer thickness in patients with vitamin B12 deficiency using spectral domain optical coherence tomography. *Curr Eye Res* 2013; 38: 680-684.

Uzawa A, Mori M, Arai K *et al.* Cytokine and chemokine profiles in neuromyelitis optica: significance of interleukin-6. *Mult Scler* 2010; 16: 1443-1452.

Van Wagoner NJ, Benveniste EN. Interleukin-6 expression and regulation in astrocytes. *J Neuroimmunol* 1999; 100: 124-139.

Waters PJ, McKeon A, Leite MI *et al.* Serologic diagnosis of NMO: a multicenter comparison of aquaporin-4-IgG assays. *Neurology* 2012; 78: 665-671.

Weinshenker BG, Wingerchuk DM, Vukusic S *et al.* Neuromyelitis optica IgG predicts relapse after longitudinally extensive transverse myelitis. *Ann Neurol* 2006; 59: 566-569.

Weis J, Katona I, Muller-Newen G *et al.* Small-fiber neuropathy in patients with ALS. *Neurology* 2011; 76: 2024-2029.

Wingerchuk DM, Banwell B, Bennett JL *et al.* International consensus diagnostic criteria for neuromyelitis optica spectrum disorders. *Neurology* 2015; 85: 177-189.

Wingerchuk DM, Hogancamp WF, O'Brien PC, Weinshenker BG. The clinical course of neuromyelitis optica (Devic's syndrome). *Neurology* 1999; 53: 1107-1114.

Wingerchuk DM, Lennon VA, Lucchinetti CF, Pittock SJ, Weinshenker BG. The spectrum of neuromyelitis optica. *Lancet Neurol* 2007; 6: 805-815.

Wingerchuk DM, Lennon VA, Pittock SJ, Lucchinetti CF, Weinshenker BG. Revised diagnostic criteria for neuromyelitis optica. *Neurology* 2006; 66: 1485-1489.

Wingerchuk DM, Weinshenker BG. Neuromyelitis optica (Devic's syndrome). *Handb Clin Neurol* 2014; 122: 581-599.

Wuerfel J, Sinnecker T, Ringelstein EB *et al.* Lesion morphology at 7 Tesla MRI differentiates Susac syndrome from multiple sclerosis. *Mult Scler* 2012; 18: 1592-1599.

Yamashita T, Miki A, Iguchi Y, Kimura K, Maeda F, Kiryu J. Reduced retinal ganglion cell complex thickness in patients with posterior cerebral artery infarction detected using spectral-domain optical coherence tomography. *Jpn J Ophthalmol* 2012; 56: 502-510.

Young KL, Brandt AU, Petzold A *et al.* Loss of retinal nerve fibre layer axons indicates white but not grey matter damage in early multiple sclerosis. *Eur J Neurol* 2013; 20: 803-811.

Zhang H, Bennett JL, Verkman AS. Ex vivo spinal cord slice model of neuromyelitis optica reveals novel immunopathogenic mechanisms. *Ann Neurol* 2011; 70: 943-954.